RECOVERY BOILER HANGER ROD ARRANGEMENT

Lappeenranta–Lahti University of Technology LUT

Master's Programme in Mechanical Engineering, Master's thesis

2022

Nikoteemu Paananen

Examiners: Professor Timo Björk

Antti Ahola, D.Sc. (Tech.)

ABSTRACT

Lappeenranta–Lahti University of Technology LUT

LUT School of Energy Systems

Mechanical Engineering

Nikoteemu Paananen

Recovery boiler hanger rod arrangement

Master's thesis

2022

90 pages, 45 figures, 3 tables and 4 appendices

Examiners: Professor Timo Björk and Antti Ahola, D.Sc. (Tech.)

Keywords: boiler fouling, bolted joint, loosening, recovery boiler, static indeterminacy, suspended structure

The thesis studied an Andritz recovery boiler's superheater support structure which involves suspending the superheaters from hanger rods which are tightened so that loads are distributed evenly. In the studied construction the rods were arranged such that the structure was statically indeterminate, and in addition depending on the tensioning condition of each rod, the balancing of loads was affected. This had resulted in inaccuracy determining the location where rods had become loose or had increased load due to ash weight of soot deposits on the superheater. A literature review was conducted to study the loosening phenomena of bolted joints. For the hanger rods, elastic interaction, differential thermal expansion and relaxation in the structure were found to result in changes to the tension condition. Based upon the findings, the static indeterminacy, effect of tightening sequence and torque on load, and thermal effects on the structure were analyzed using Ansys Mechanical 2022 R1 finite element analyses. The findings of the analyses were used to list possible improvements to the structure so that the hanger rod loads would be verifiable more accurately. These involved suggestions on what changes to the structure are most effective in reducing its static indeterminacy, how using certain tightening sequences with tailored preload values result in an evenly distributed load on the hanger rods, and how the thermal effects in the structure should be considered.

TIIVISTELMÄ

Lappeenrannan–Lahden teknillinen yliopisto LUT

LUT Energiajärjestelmät

Konetekniikka

Nikoteemu Paananen

Soodakattilan kannatustankojen asettelu

Diplomityö

2022

90 sivua, 45 kuvaa, 3 taulukkoa ja 4 liitettä

Tarkastajat: Professori Timo Björk ja TkT Antti Ahola

Avainsanat: kattilan likaantuminen, löystyminen, pulttiliitos, riippuva rakenne, soodakattila, staattinen määräämättömyys

Työssä tutkittiin Andritzin soodakattilan tulistimen kannakointia, jossa tulistimet ripustetaan tangoista, jotka kiristetään niin, että kuormat jakautuvat tasaisesti. Tutkitussa rakenteessa tangot oli järjestetty siten, että rakenne oli staattisesti määrittämätön, lisäksi kunkin tangon kiristystilanne vaikutti kuormien tasapainoon. Tämä johti epätarkkuuteen määriteltäessä paikkaa, missä tangot olivat löystyneet tai kuormitus kasvanut johtuen tulistimeen kohdistuvasta tuhkapainosta. Kirjallisuuskatsaus tehtiin ruuviliitosten löystymisilmiöiden tutkimiseksi. Ripustustankojen tapauksessa elastisen vuorovaikutuksen, epätasaisen lämpölaajenemisen sekä rakenteen jäykkyyden vähenemisen lämpötilan kasvaessa havaittiin johtavan muutoksiin jännitystilassa. Havaintojen perusteella analysoitiin staattista määräämättömyyttä, kiristyssekvenssin ja käytettyjen kiristysvoimien vaikutusta kuormituksen jakautumiseen tangoille, sekä lämmön vaikutuksia rakenteeseen Ansys Mechanical 2022 R1 elementtimenetelmällä. Analyysien tulosten perusteella listattiin mahdollisia parannuksia rakenteeseen niin, että ripustustankojen kuormat olisivat todennettavissa tarkemmin. Nämä sisälsivät ehdotuksia siitä, mitkä rakenteen muutokset vähentävät tehokkaimmin sen staattista määräämättömyyttä, kuinka tiettyjen kiristyssekvenssien käyttö räätälöidyillä esikuormitusarvoilla mahdollistaa kannatustankojen tasaisesti jakautuneen kuormituksen ja miten lämmön vaikutukset tulisi ottaa huomioon rakenteessa.

SYMBOLS AND ABBREVIATIONS

COF	Coefficient of friction	
FEA	Finite element analysis	
FEM	Finite element method	
PWHT	Post weld heat treatment	
SH rod	Superheater hanger rod	
D	Major diameter	
E	Young's Modulus	
F	Load	
G	Shear modulus	
J	Torsional constant	
K	Experimentally defined nut factor	
L	Length	
T	Torque	
α	Coefficient of thermal expansion	
θ	Angle of torsion	[rad]
μ	Linear density	
ρ	Density	

Table of contents

Appendices

Figures

Tables

1 Introduction

A recovery boiler is an integral part of the pulp mill, where its function is to burn organic material dissolved in black liquor in order to recover and reuse the spent cooking chemicals. The burning of black liquor generates high pressure steam which can then be utilized as process steam or in electricity production. (Vakkilainen 2005)

Modern recovery boilers are totally self-sufficient, meaning that the energy released from burning black liquor can cover even the whole pulp mill's process needs fully. The excess energy can then be used in for example district heating and electricity production into the power grid. Metsä Fibre, a pulp mill operator claims that its mills had an energy self-sufficiency rate of 151 percent in 2021. (Metsä Fibre 2022)

The burning of black liquor in the recovery boiler generates flue gases that contain ash. The ash then accumulates on the various heat transfer surfaces (superheaters, boiler bank, economizers) as it traverses through the boiler. This accumulation of ash on the heat transfer surfaces acts as an insulant lowering their heat transfer capacities, thus requiring a system for removing ash deposits in order to maintain optimum performance of the boiler. Sootblowers are the most common method in today's recovery boilers for cleaning the accumulated ash off the heat transfer surfaces. (Pöllänen 2019)

The removal of deposits via sootblowing consumes steam and causes fatigue loading on the heat transfer surfaces, which is why conducting the process only where/when it is needed improves the overall boiler efficiency and reduces fatigue (Pöllänen 2019). To achieve this, Clyde Bergemann, a sootblower manufacturer was one of the first to start experimenting with a method of determining the need for sootblowing via ash weight imposed on heat transfer surfaces (Wicker 2003).

1.1 Background and motivation

This thesis is commissioned by Andritz. In a recovery boiler, the heat transfer surfaces are suspended from the boiler steel structure via hanger rods. To determine the location where sootblowing is required, Andritz uses strain gauges based on Pöllänen (2019, pp. 39-50) as a part of its smart recovery boiler solution to measure changes in the load on each hanger rod. By comparing the measured strain with the calibrated weight of the hanged elements, the weight change caused by contaminants/condensates can be acquired. The problem in this method is that in the current construction the rods are arranged such that the structure is statically indeterminate, and in addition depending on the tensioning condition of each rod, the balancing of loads is affected. This results in inaccuracy determining the location where rods are loose or sootblowing is needed.

1.2 Research problem

The static indeterminacy of the hanger rod arrangement in the superheaters' case is due to the elements being welded to the furnace roof and superheater headers, while also being suspended from smaller hanger rods which are then connected to intermediate beams via bolted joints. These are then suspended via larger hanger rods (on which the strain gauges are located) from the tertiary boiler beams creating another bolted connection. The construction in question is shown in Figure 1.

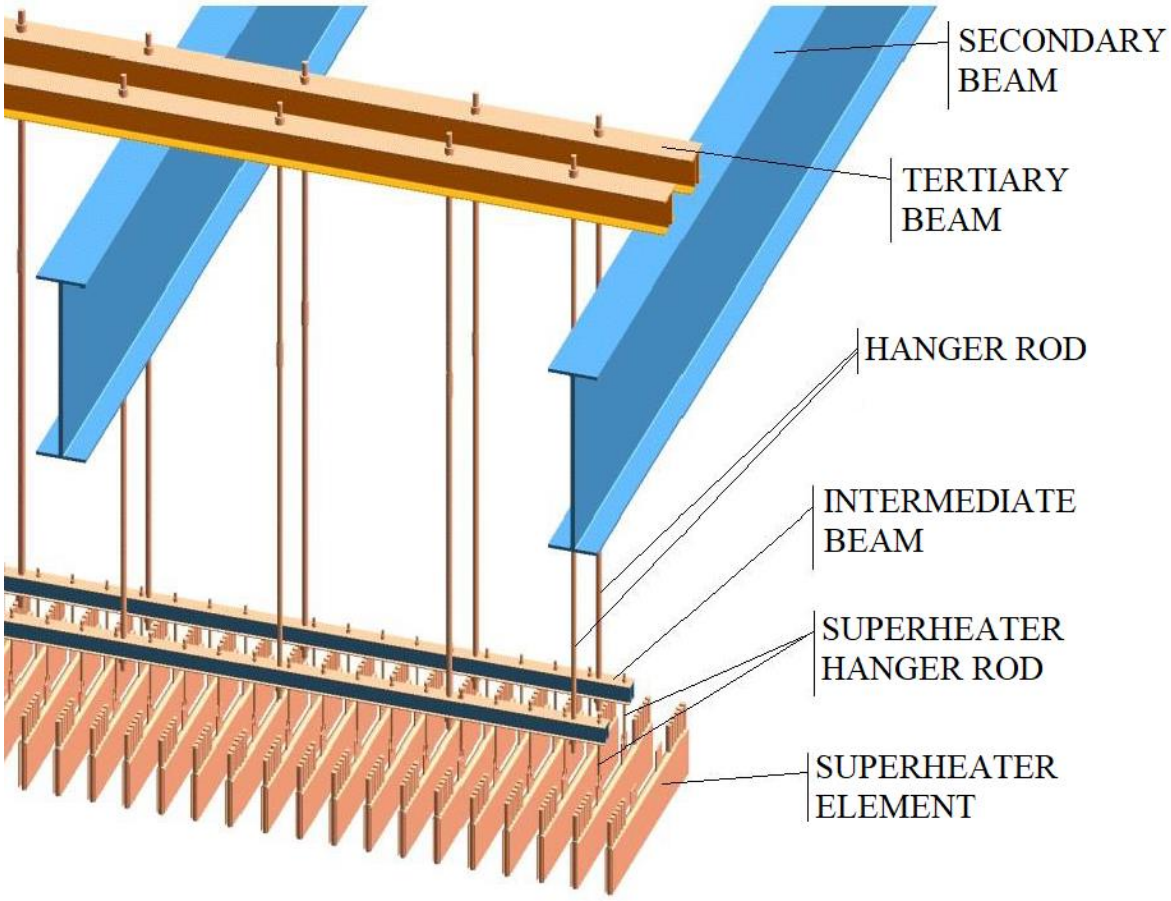

Figure 1. Hanger rod construction of a superheater stage in an Andritz recovery boiler. Strain gauge system, headers, and furnace roof not shown.

The rods are tightened during installation, but there have been problems regarding the uniformity of tension between them. This can result in some hanger rods being loose, thus causing multiple problems such as:

- Excessive swinging of elements inside the boiler.
    - Risk of collision to other elements or sootblowing lances.
    - Fatigue of support box connection to furnace roof and welded connections between superheater piping and header.
- Causing issues when using the strain gauge system for measuring ash weight.
- Additional stress induced to furnace roof, increasing instability/yielding risk.

Determining a way of making sure the tensioning stays within acceptable limits and the load changes can be measured accurately using the strain gauge system during boiler operation is essential.

1.3 Objective

The objective of the research is finding out different phenomena affecting the hanger rods, and based on findings, listing the necessary changes required to better ensure their loading condition.

1.3.1 Research questions

Multiple research questions are formed from the research problem.

- What causes preload loss of hanger rods post-tensioning?
    - What kind of effect does the tightening sequence have on post-tensioning condition?
    - What kind of effect does the stiffness of the tertiary beams and intermediate beams have on post-tensioning condition?
- How does the penthouse environmental condition affect the hanger rods?
- How should a structure where the load on each hanger rod is verifiable be created?

1.3.2 Hypotheses

Based on the research questions, the following hypotheses are formulated:

- Suspending each superheater element from the hanger rods causes deflection in the supporting beams, which will gradually increase with more elements being suspended / rods tightened as assembly proceeds. The beams thus deflect from under the nut, causing relaxation of the bolted joint.

- In addition to ensuring the tension condition of each hanger rod, to better extrapolate the horizontal location of soot deposits on superheater elements from the load in the hanger rods measured via the strain gauge system, the hanger rod structure's static indeterminacy needs to be reduced.

Considering the above listed hypotheses, determining ways of both controlling the beam deflection for achieving the most optimal condition post-tensioning and achieving static determinacy of the hanger rods should be paramount for solving the research problem.

1.4 Research methods

The research is divided into two phases. First, a literature review is conducted into earlier research regarding bolted joints to gain an understanding of the interactions between different variables in the hanger rod structure that cause unevenly distributed loads. Andritz's experiences and data regarding the currently in use construction is also collected.

In the second phase the construction is tested with Ansys Mechanical 2022 R1 finite element analysis (FEA) by simulating the loading condition during installation. The order of tightening, different tightening torques, and penthouse environment effect on the tension condition of the hanger rods is examined.

The findings of both phases are used for listing methods for the hanger rod structure so that the hanger rod load is verifiable more accurately.

1.5 Scope and contribution

The scope of the study is limited to the hanger rods suspending the superheaters to control the workload. Other parts hanged via hanger rods include the boiler walls, economizers, and boiler bank. The solutions from studying the superheaters should be applicable in part to the

other heat transfer elements as well. FEA are conducted only on a single superheater to manage the work and computational load of the analyses.

Research on the topic of bolted joints mostly deal with the traditional connection, where the connected elements come into contact with each other as a result of tightening. In the hanger rod application this is not the case, which is why the thesis contributes to research by studying the interaction of bolted joints with long distance between ends subjected to high temperatures.

Achieving the goal of the thesis would enable the improved use of sootblowing optimization resulting in less steam consumption and thus better efficiency of the boiler, so there is also an economical and environmental contribution.

2 Loosening of bolted joints

To ensure the tension condition of the hanger rods, their loosening phenomena must be understood. This section deals with the loosening of bolted joints and the unique considerations that need to be accounted for when dealing with the hanger rod application. Data provided by Andritz is used to find out the conditions the hanger rods are subjected to, and scientific literature is reviewed to understand what can be done to compensate for them.

The latest review of loosening related research, Gong et al. (2021) examined research on the loosening phenomenon and defined the loosening of bolted joints as the loss of preload in the joint. Furthermore, it partitioned the loosening phenomena into rotational related, and non-rotational related loosening, while prior reviews have mostly dealt with the vibration induced dynamic load dependent rotational loosening (Kakirde & Dravid 2017; 2018). The difference between the rotational and non-rotational loosening is that non-rotational loosening deals with the loss of preload in the joint that happens even though the nut does not rotate. Figure 2 lists the different causes related to both types of loosening.

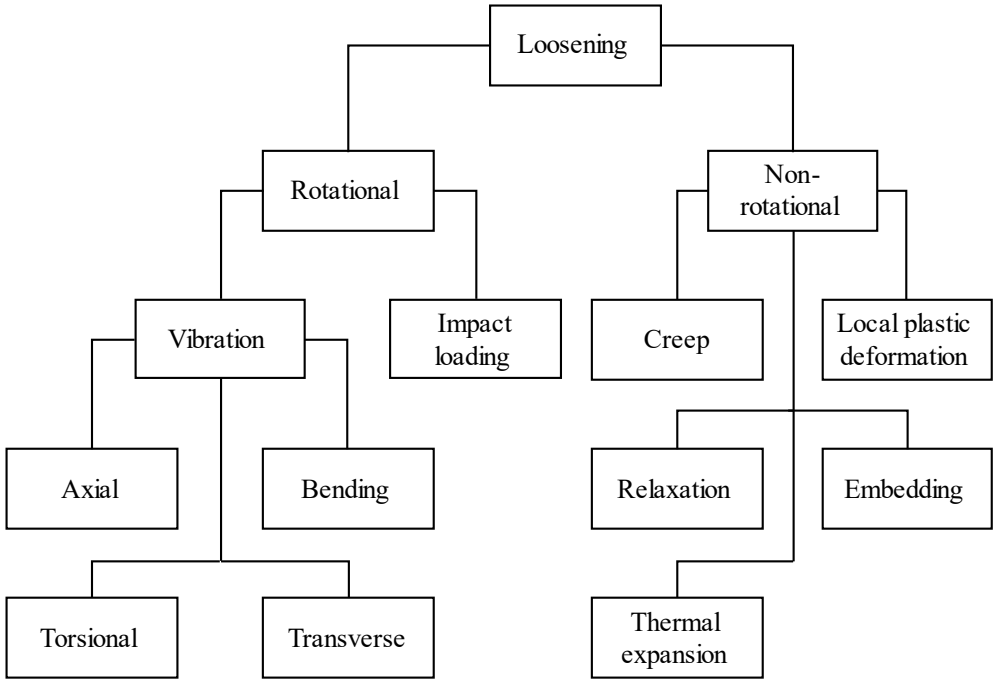

Figure 2. Overview of the causes for bolted joint loosening.

Each cause of loosening seen in the figure is the result of an underlying application specific phenomenon, usually a combination of multiple phenomena (Gong et al. 2021). Later in the section, an overview of the hanger rod application related potential causes for loosening will be examined.

2.1 Rotational loosening

Rotational loosening can be identified by measuring the angular displacement of the nut compared to its post-tightening position. It can also be noticed by measuring the change in the thread protrusion length before retightening. Angular displacement of the nut occurs when the friction between nut–bolt threads or nut–part surface is overcome by an external force, be it from vibration (Li Z. et al. 2021) or impact loading, thus making it a dynamic load dependent phenomenon.

2.1.1 Vibration

The experiments done by Junker (1969), where a transverse vibration test machine was used to test the transverse vibration effects on bolts for the first time, implicated that this type of vibration caused a visible rotation of the nut and thus a large loss of preload. The effect of rotational loosening under vibration is dependent on the vibration type, amplitude, number of vibration cycles, and initial bolt preload. The effect of vibration frequency has been found to have no effect when studying the amount of preload loss per vibration cycle. (Li Z. et al. 2021, pp. 13-14).

Using the torque method to tighten the nut causes torsion of the bolt owing to the friction between the threads of the bolt and the nut, which results in residual torque stress on the bolt shank (Hess 2022). Under the cyclic nature of transverse vibration, the residual stress can be slowly released by rotation of the nut, loosening the joint (Kasei et al. 1988).

$$\theta = \frac{TL}{JG} \tag{1}$$

Equation (1) from Bird & Ross (2020, p. 162-163) shows that the torsion in response to a specific torque is dependent on the length of the bolt shank, thus increasing the length of a bolt makes it more susceptible to this phenomenon. In the equation, θ = torsion [rad], T = torque, L = length, J = torsional constant, and G = shear modulus. Hess (2022) found that when tensioning a bolted joint using hydraulic tensioning, the torsion could be completely avoided. When utilizing this method contrary to the torque method, inducing a slip between the nut and part surface required more than five times larger external loading. This is due to the method not causing torsion of the bolt shank.

The effect of axial vibration on rotational loosening has been controversial in the past owing to probably measurement methods being less accurate (Gong et al. 2021, pp. 340-342). With the advances in research methods, relatively recent findings have concluded that axial

vibration does not result in rotational loosening, instead it is thought to cause non-rotational loosening via coefficient of friction (COF) dependent wear (Liu et al. 2015; Liu et al. 2017), or plastic deformation (Nassar et al. 2011; Yang et al. 2012) of the connected surfaces.

2.1.2 Impact loading

Rotational loosening has been found to occur when the joint is subjected to a transient high speed external loading, which is classified as impact loading. The resulting loosening has been found to be dependent on the number of impacts and their amplitude. The direction of the load against the bolt axis and the frequency of the impacts have been found to have no effect on the amount of preload loss. The effect of impact loading on loosening is very similar to vibrational loading, the difference being that impact occurs fast and could often be an unpredictable phenomenon, while vibration is more constant and predictable during the life of the joint. (Gong et al. 2021, pp. 346-347)

2.1.3 Prevention of rotational loosening

To prevent rotational loosening, different methods to reduce the nut's ability to rotate can be employed. The friction coefficient can be controlled by material selection or by employing different thread locking compounds, and adhesives (Gong et al. 2022, pp. 53-54), higher COF having better loosening resistance. Its dependence on temperature should also be taken into account as was found by Pearson et al. (2013) where the decrease of COF was observed when heating high-strength steel from 24 °C to 450 °C. The decrease was found to be proportional to sintering of oxide particles on the material surface. Additionally, if grease is used to protect the threads for PWHT (post weld heat treatment) and shipping, its effect on the COF and thus loosening must be considered.

By placing bolts where they experience less temperature (for example, protecting bolts from heat with insulation) and vibration (placing bolts nearer to rotational centres, using dampeners to lessen the effects of vibration), risk of rotational loosening can be reduced.

Using different tightening methods such as the hydraulic tensioning can improve the resistance against rotational loosening through improving the residual stress condition of the joint. There are also different kind of locking nuts and washers designed to combat thread and bearing surface slippage, while using the double-nut method can also be an economical way to achieve similar anti-loosening performance as locking nuts (Gong et al. 2022, pp. 50-53).

The double-nut consists of a thick nut and a slimmer nut which is called the jam nut. The proper installation requires that the slimmer nut is tightened first against the bearing surface to about 25-50% of the desired preload, after which the thicker nut is tightened on top of the jam nut while its rotation is prevented until the desired preload is reached in full. If using long bolts, a thin nut cannot be used as it would be susceptible to thread stripping. The double-nut has poorer anti-loosening properties against vibration and impact loading if not properly installed. The proper installation process is time consuming and requires a skilled operator. (Bolt Science 2021c; ISO 898-2:2012)

2.2 Non-rotational loosening

Non-rotational loosening happens when preload is lost without the nut rotating. This can be as consequence of the bolt's elongation due to various reasons, or deformation/deflection of the parts connected by the bolt. This kind of loosening can be identified if a change in length of the bolt is observed, or if by after retightening, the protrusion length of the thread has increased.

2.2.1 Elastic interaction and thermal relaxation

Elastic interactions between bolts result in relaxation of the preload, which is dependent on the tightening sequence and causes most of the unevenness seen in the preload distribution (Abasolo et al. 2011; Li Y. et al. 2019). A lot of experiments have been done on optimal tightening sequence of gasketed flanged joints, where the gaskets are soft to achieve a sealed

connection and thus also gasket deformation induced relaxation occurs when tightening. In the studies, the elastic interaction coefficients of the joints were obtained experimentally based on which improved bolt-up procedures were devised which could achieve only ±2% variance of the preload distribution between bolts (Bibel & Ezell 1992; Goddard & Bibel 1994; Bibel & Ezell 1996). Wang Y. et al. (2017 pp. 307-308) analysed a linear multi-bolted joint and found that the relaxation depends heavily on the elastic interaction stiffness of the joined parts, which is showcased in Figure 3 where the stiffness of the bearing surface between bolts 1 and 2 is idealized as a spring with stiffness K_{12}.

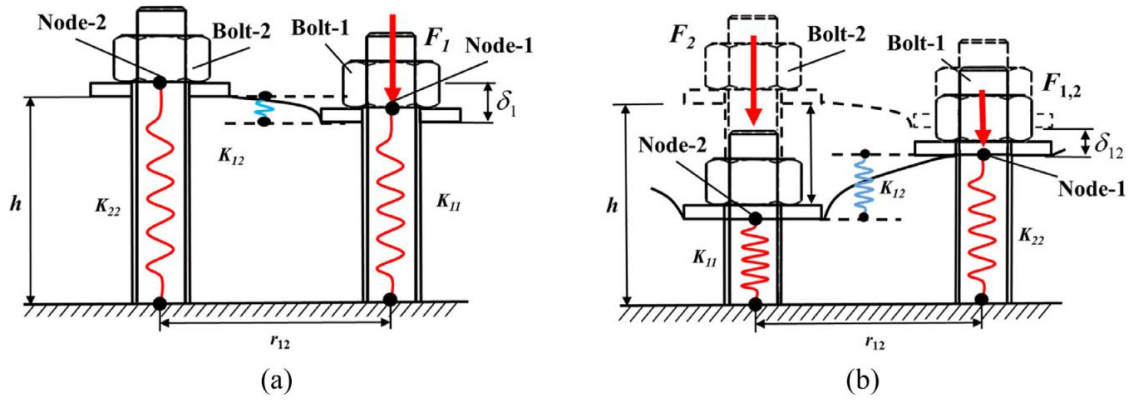

Figure 3. Demonstration of elastic interaction in a 2-bolt joint when (a) tightening bolt 1 and (b) tightening both bolts sequentially. (Wang et al. 2017, p. 309)

To achieve a uniform preload, the elastic interactions of the joint corresponding to different tightening sequences must be estimated after which, through understanding of the elastic interactions, the required tightening for each bolt in the sequence can be calculated, which would ideally result in the desired preload condition after the tightening sequence is completed (Bibel & Ezell 1992; Goddard & Bibel 1994; Bibel & Ezell 1996). The elastic interaction behaviour in the hanger rods could also be analysed experimentally like in the research mentioned previously, though it would obtain solutions applicable only to a specific boiler, and the large number of bolts in the structure would make conducting it very slow and costly.

With the advances in computation, nowadays the tightening sequence could also be optimized using computer aided simulation such as the finite element method (FEM), though this would be computationally demanding as the analysis would have to be conducted again in every step of the tightening sequence (Abasolo et al. 2011). To save on costly computational or experimental analysis Abasolo et al. (2011) developed a metamodel which is composed of four different parameters and could be used to simulate the elastic interaction behaviour of the joint. After the parameters were validated through FEA, a MATLAB algorithm was produced, which was used for reproducing the elastic interaction of various tightening sequences, using significantly less computational resources. Although the metamodel was developed for a bolted flange joint of a wind turbine tower, the authors claimed that the method would be usable for any bolted joint.

The studies mentioned in this section were conducted on bolted joints where the connected elements are brought into contact with each other by the bolts. As the hanger rods are instead used to suspend the superheaters, their elastic interactions act differently, and the effect of deflection is more pronounced in variance of the preload distribution, which results in nonlinear behaviour of the structure and would thus invalidate the methods for optimising the tightening sequences that have been produced in former research. This is because stiffness K_{12} shown in Figure 3 would be much lower as instead of stiffness arising from compression resistance of the connected parts, it is instead related to the deflection of the beams, which is dependent on distance between supports and the stiffness of the beams.

The relaxation of bolted joints can also be seen after tightening if the temperature is increased. Kim et al. (2012) compared properties of different stainless steel grades from multiple sources, out of which the dependence of Young's modulus (ratio of stress to strain) to temperature can be seen in Figure 4. The scatter in the data was claimed to be due to differences in test conditions and material properties.

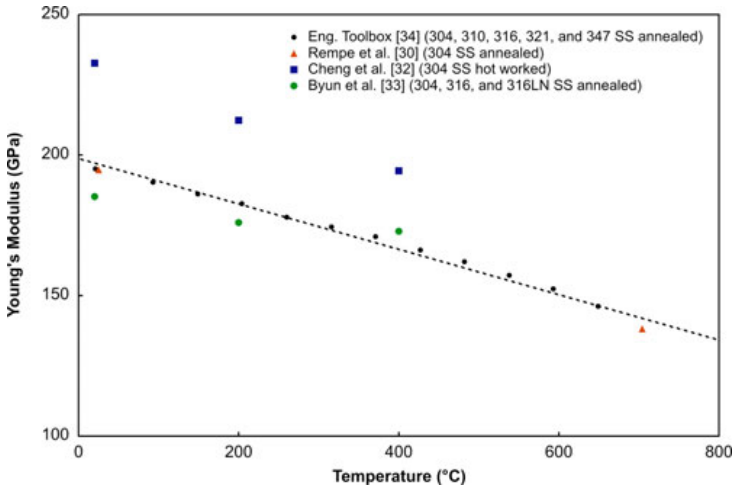

Figure 4. Young's modulus' dependence on temperature of various stainless steel grades. (Kim et al. 2012, p. 422)

As the Young's modulus decreases in response to increasing temperatures (Kim et al. 2012; Bolt Science 2021b), following Hooke's law, the elastic stress required to maintain the strain from preloading will lower. This causes temporary loosening of the bolted joint, which can be reversed if it is cooled back to the original temperature. In addition to this phenomenon, the effect of thermal expansion further affects the preload condition in response to a change in temperature. This is examined in a separate section.

2.2.2 Embedding

Materials are never completely smooth, therefore the unevenness resulting from the surface roughness of connected parts causes stress concentrations at the peak points of the surface. Some plastic deformation at the point of the stress concentrations will always occur on contacting surfaces shortly after the nut is tightened, and a part of the preload is lost. (Bolt Science 2021a; Jaglinski et al. 2007, p. 51; Bickford 1995). Under static loading, most of the embedding loss occurs a few minutes after tightening (Jaglinski et al. 2007, p. 51; Bickford 1995).

However, further loss of preload is accumulated as the bolted joint experiences external loading after assembly. Therefore, manufacturers often recommend a break-in period for products after which the tightness of bolts is examined and retightened to the specified preload if necessary. In some applications this kind of retightening is not possible, so the embedding should be taken into account already in the design phase. Longer bolts are more resistant to this kind of preload loss due to the displacement being unaffected as bolt length is increased, while the displacement to preload loss ratio decreases. Distributing the stress using a wider and thicker washer or baseplate also reduces the amount of embedding due to decrease in contact stress. (Bolt Science 2021a)

2.2.3 Local plastic deformation

Discontinuities in the bolted joint cause local stresses which might exceed the yield limit of the material. In static loading these will plasticize locally and achieve equilibrium, but as cyclic loading is applied in the way of mechanical or thermal stress, progressive accumulation of plastic deformation (also known as ratcheting) will occur. As the bolted joint experiences local yielding, preload is lost. Jiang et al. (2019) found that cyclic torque loading induced ratcheting at the root of the threads of a curvic coupling bolted joint and caused a decrease in preload. If yielding causes strain-hardening in the material, after a certain number of loading cycles the preload reducing effects of the phenomenon will diminish.

In the case of the hanger rods there is potential for local plastic deformation as the rods have discontinuities in the way of threads and sleeves for connecting riser piping support beams. In addition, the rods experience thermal stresses during boiler start-up and shutdown. Further cyclic loading might result from seismic activity if the boiler is located at a seismic zone.

2.2.4 Creep

Creep is experienced as thermal energy reduces the amount of stress needed for dislocations to occur in the material's grain boundaries, loading therefore starts to cause plastic strain. Although creep occurs at any temperature with the rate at which it occurs increasing with temperature and stress, depending on the source, at temperatures higher than 40-50% of the material's melting point (in Kelvin), the plastic deformation under constant stress as a function of time can be considered a potential cause of failure (Kassner 2009; González-Velázquez 2020). Figure 5 shows how creep-induced strain occurs over time under constant stress and temperature.

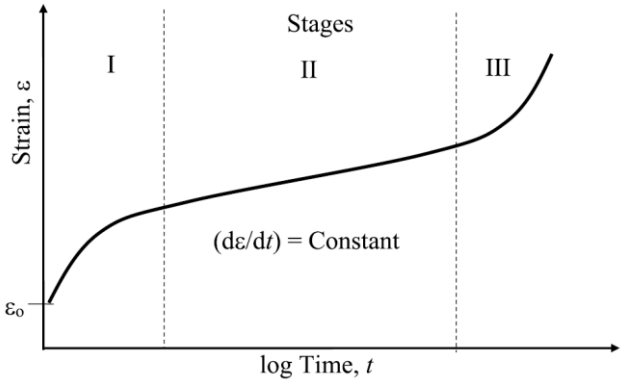

Figure 5. The plastic strain caused by the three stages (primary, secondary, and tertiary) of creep idealized at constant stress and temperature over time. (González-Velázquez 2020, p. 228)

As can be seen in the figure, creep starts as the loading is applied and leads to a relatively fast initial strain in the primary stage, after which the strain will keep increasing at a constant rate as a constant load is applied in the secondary stage, also called steady-state creep. If the temperature and loading is high enough relative to the material's creep resistance, the phenomenon will eventually lead into rupture at the tertiary stage. (Kassner 2009; González-Velázquez 2020)

In bolted connection loosening, the loss of preload caused by creep deformation of the bolt and gasket is much more prevalent than creep rupture induced bolt fracture (Nechache & Bouzid 2007). As most of the creep life is under steady-state creep, it's the most vital for estimating loosening under the phenomenon (Kassner 2009, p. 9). For calculating creep elongation, a couple of methods have been developed such as the theta projection method (Evans & Wilshire 1993) and Wilshire method (Wilshire & Battenbough 2007).

As creep is dependent on stress, temperature, and time, creep-caused deformation is especially relevant in materials that are subject to high temperatures for extended periods and have discontinuities causing local stresses. In the case of hanger rods, which are located in the penthouse which has temperatures ranging from 300 °C to 400 °C while the boiler is operational, creep induced elongation of rods can happen, affecting their load distribution over time.

2.2.5 Thermal expansion

When materials are heated, they will expand, and when they are cooled, this expansion is reversed. The phenomenon is connected to material dependent thermal expansion coefficients which are constant in response to temperature for most solids. (Bird & Ross 2020, p. 296-297)

After being tightened in ambient temperatures, if during operation the bolted joint experiences a temperature gradient or has materials with differing thermal expansion coefficients, the components will experience differing amounts of thermal expansion. As a result, there will be a change in the joint's preload condition. (Sears & King 2004). This can lead to loosening if for example the bolts are exposed to an unequally distributed temperature, like in the case of the hanger rods. Conversely, if retightening is conducted at the elevated temperature when this kind of loosening is noticed, after temperature cools down at for example boiler shutdown and thermal shrinkage occurs, the tension condition will change again.

2.2.6 Prevention of non-rotational loosening

To summarise the findings from literature regarding the non-rotational loosening phenomena, the different kind of dependencies of each phenomenon and methods to reduce effects of the related loosening are compiled and shown in Table 1.

Table 1. Non-rotational loosening prevention methods.

	How to prevent
Relaxation (Abasolo et al. 2011; Wang et al. 2017; Li Y. et al. 2019; Bolt Science 2021b)	• Using optimized tightening sequences to control elastic interaction induced relaxation • Increasing elastic interaction stiffness of connected elements • Compensation of thermal relaxation by increased preloading
Embedding (Bickford 1995; Jaglinski et al. 2007; Bolt science 2021a)	• Using longer and wider bolts or otherwise reducing contact stresses by distributing them on a wider area • Higher surface quality of connected surfaces
Local plastic deformation (Jiang et al. 2019)	• Have the joint experience cyclic loads that remain under the ratcheting limit • Less discontinuities / reducing stress concentrations at discontinuities through smoother geometry etc.
Creep (Kassner 2009; González-Velázquez 2020)	• Material selection for higher creep resistance • Reducing temperatures experienced by the joint • Lower stresses in the joint by having larger cross sections, less discontinuities / reducing stress concentrations at discontinuities through smoother geometry etc.
Thermal expansion (Sears & King 2004; Bird & Ross 2020)	• Control of thermal expansion coefficients via material selection so that differential thermal expansion can be avoided • Having an evenly distributed temperature throughout the joint

2.3 Hanger rods

What makes the hanger rod application quite unique at least in Andritz's case is that the rods generally have a long distance (7 – 12 m) between ends. Furthermore, the rods are divided by the penthouse insulation into an upper section which is outside the insulation and thus experiences lower temperatures, and a lower section which is inside the penthouse and subjected to much higher temperatures. This division by the insulation layer is showcased in Figure *6*.

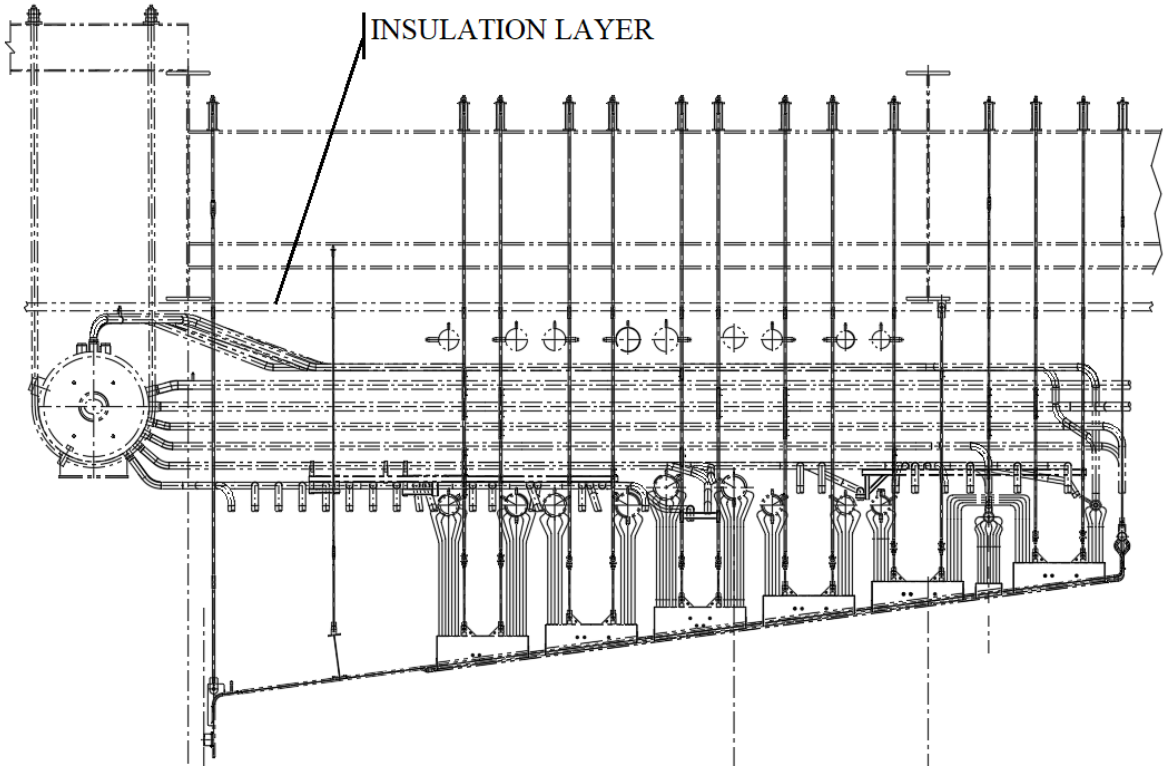

Figure 6. Side view of the superheater hanger rods with insulation divide visible. Courtesy of Andritz.

If the boiler is built on a seismic zone, then there will be the possibility of an earthquake occurring during operation. This will cause cyclic loads on the hanger rods and could thus lead to dynamic load dependent loosening of the bolted connections.

$$T = KFD \quad (2)$$

According to Bickford (1995), to achieve a specific preload in the bolt when using the torque tightening method, the required torque can be calculated with equation (2), where *T* is the torque applied, *K* is the experimentally defined nut factor, *F* is the bolt preload, and D is the major diameter of the bolt. The torque method has inaccuracy due to the thread and surface friction taking ~80% of the applied torque while only ~20% (depending on the nut factor which is affected by used material, lubrication, surface quality, etc.) goes towards the bolt's preload. (Bickford 1995). Whereas using hydraulic bolt tensioning allows bypassing the inaccuracy.

$$f = \frac{1}{2L}\sqrt{\frac{F}{\mu}} \quad (3)$$

The rods are exposed between ends, therefore their tension can be accurately measured using percussion-based methods such as Wang F. & Song (2020). Mersenne's laws dictate that a string's frequency is dependent upon its tension, thus Equation (3) for the hanger rods, where *f* is the frequency, *L* the length of the rod, *F* is the tension, and μ is the linear density of the rod. A skilled operator can notice these differences in the tension condition just by ear, enabling fast checks on the tension condition after a seismic event for example. For accurate measurements however, methods such as the one mentioned above should be considered.

2.3.1 Elastic interactions

Due to the nature of the entire furnace's vertical constraint being achieved by it being suspended from hanger rods, when a hanger rod is tightened—in order to maintain static equilibrium, the increased tension has to be brought to the tightened rod via the elastic interaction induced stress redistribution of the other hanger rods, loosening them. Figure 7 shows an idealized example about how stress redistribution occurs when tightening the rods.

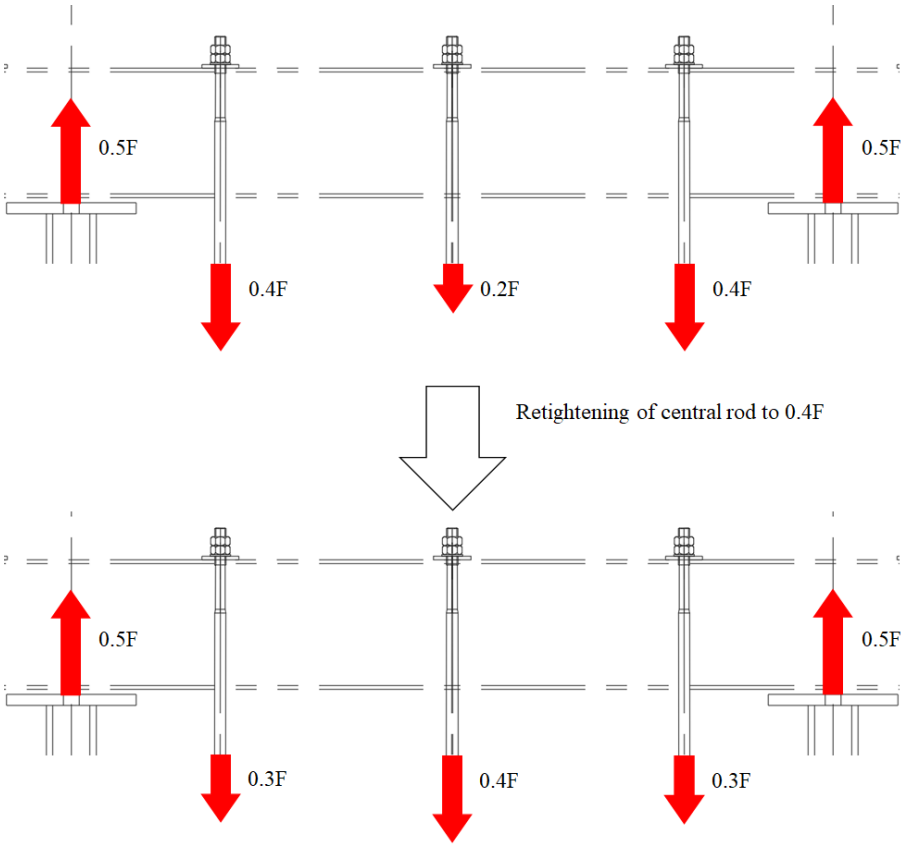

Figure 7. Example about stress redistribution in hanger rods after tightening.

As hypothesised in the introduction chapter and based on the findings of the literature review, the resulting loosening depends upon the stiffness of the hanger rod supporting beam structure, length of the beams, and proximity of the other rods. If during boiler operation all the rods were to stretch equally, no redistribution of stresses would occur and thus no loosening would be perceived. The fact that rods have been noticed to become looser compared to their neighbouring rods reveals that there must be some unequally distributed phenomenon which results in loosening over time.

To reliably approximate the ash weight locations on superheaters from the hanger rod strains, a uniform stress distribution between the rods needs to be achieved (Pöllänen 2019, p. 49). In the hanger rod case, as the joined parts—furnace roof and tertiary beam are not in direct contact with each other, deflections are expected, which results in a high variance of the

tensioning condition. Andritz's tension assessment of rods during boiler shutdown have found that the rods generally have higher tension near the side walls, while nearer to the centre of the penthouse, rods are looser.

Later in the numerical analysis part of the thesis, the effect of the stress redistribution and if it can be controlled by utilizing different tightening sequences to achieve better uniformity in the tension is studied using FEA. The current Andritz solution utilizes the torque method for tightening. As was found from the literature, this causes elastic torsion because of thread friction torsional stress and as the hanger rods are long, they are more susceptible to it. Simultaneous tightening of multiple bolts is possible by using hydraulic tensioning instead (Sears & King 2004, p. 516), which could be a beneficial tightening method to be used if the findings of FEA determine that a more uniform stress distribution can be achieved via a certain tightening sequence. It would also negate the aforementioned torsional effects which can lead to rotational loosening of the nut through the springback phenomenon.

Swinging of superheater elements inside boiler might cause cyclic relaxation of opposing hanger rods at each superheater stage, which could result in loosening over time. However, tests done on site by Andritz have found that no movement is transmitted to the hanger rods past the superheater support box when the superheaters are swung deliberately. The swinging might instead cause fatigue of the support box–furnace roof weld and result in ash leakage from the furnace. Connecting the superheater elements together from the bottom would increase their stiffness against sootblowing, the viability of which considering the fouling of flue gas flow transverse structures could be investigated.

2.3.2 Effect of temperature

Resulting from reviewing the literature regarding bolted joint loosening, it is found that the hanger rods have three separate loosening phenomena depending on temperature. These are thermal relaxation, thermal expansion, and creep.

After boiler start-up, thermal expansion of hanger rods occurs as penthouse temperature rises. There is unevenness of temperature inside penthouse while the boiler is warming up, (thermal flux has not yet achieved static state) due to the headers radiating high heat, (>500 °C steam temperature inside of last superheater header) while the risers and roof piping have liquid water flowing inside them. This results in differential thermal expansion of the rods.

The hanger rods' lengths vary within the insulation due to inclination of the furnace roof seen in Figure 6, which is why the leftmost (when viewed from right side of boiler) superheater hanger rods experience more thermal expansion when compared to rightmost superheater if the temperature is equal. Therefore, the longer hanger rods should be tightened more compared to the shorter ones so that when differential thermal expansion occurs as the penthouse temperature rises, the load distribution evens out.

Headers are in close proximity to the hanger rods with the distance being under 100 mm. The superheating stages' headers have different temperatures, and the temperature radiating from them heat the hanger rods. This would result in differential creep deformation of the hanger rods making the stress distribution uneven.

Measurements done by Andritz on the penthouse temperature have found that there is horizontal temperature variance in the penthouse. The measurements have only been done to compare the temperatures at the superheaters and economizers, ~360 °C and ~310 °C respectively (with some variance between projects depending on boiler design values). Due to difficulties accessing the penthouse and no sensors being placed beforehand, the data is lacking. If the temperature varies between the centre of the penthouse compared to the sides so that the temperature is lower near the sides, the hanger rods' thermal expansion, possible creep, and elongation from the smaller decrease in the Young's modulus will be lower near and on the side walls compared to the centre. Thus, stress would be redistributed from the centre to the sides leading to inequal stress distribution throughout the superheater hanger rods.

Based on the findings of the literature review it is concluded that if during boiler operation the hanger rods were subjected to an identical temperature and stressed evenly, the effect of temperature on loosening would be eliminated as each rod would expand and deform equally. The sensitivity of the hanger rod structure against temperature variance will be tested in the analysis section of the thesis to determine if further temperature measurements are needed and if some kind of mixing of the air inside the penthouse or other kind of solution would be beneficial to ensure uniform temperature and thus stress distribution of the hanger rods.

3 Static indeterminacy of ash weight measurements

In this section, the static indeterminacy of the ash weight measurements in the current Andritz solution is examined more closely. Figure 8 shows how the measurements are complicated by the superheater elements having a possible load path through the furnace roof and through the intermediate beam. Also, the risers which are supported by beams connected to the hanger rods further complicate extrapolating the location of the soot deposits from the strain gauge measurements.

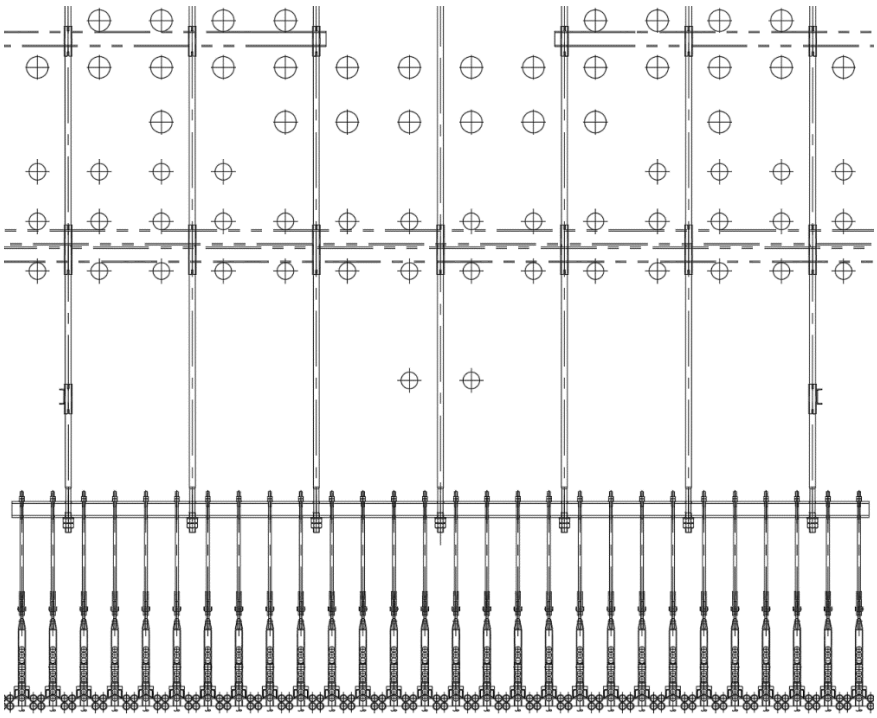

Figure 8. Sources of static indeterminacy in the superheater hanger rod construction. Hanger rods also support the risers on their way to the steam drum. Courtesy of Andritz.

As can be seen in Figure 9, the intermediate beam allows the superheaters' weight load to flow through it and distribute among the hanger rods, leading to inaccuracy when approximating the exact location of the weight change caused by ash deposits. By measuring the strains from the longer hanger rods, only the centre of the weight change can be acquired.

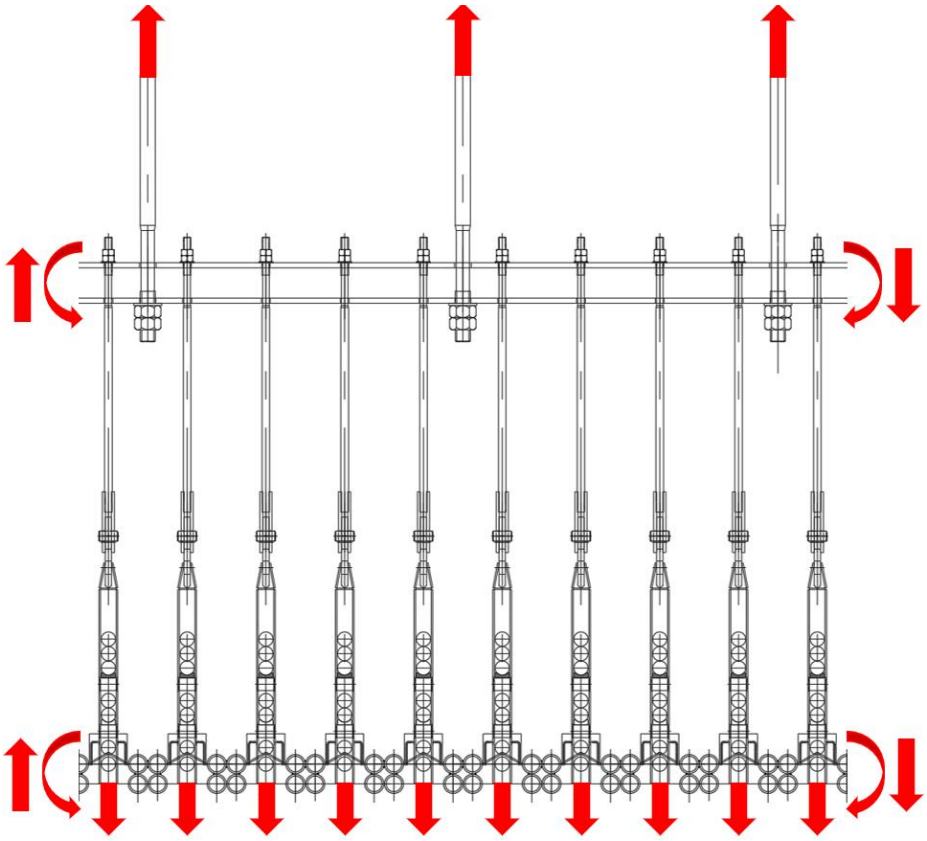

Figure 9. Static indeterminacy caused by intermediate beam and furnace roof.

If other sources of static indeterminacy were ignored, the accuracy could be improved by dividing the intermediate beams into shorter sections so that each beam is carried by two rods. This way each intermediate beam would have their own centre of weight change obtained from the longer hanger rods. However, in addition to the intermediate beam, especially if a rod has become loose, the load can also flow through the furnace roof, headers, and riser supports, adding to the weight seen by an adjacent hanger rod, thus skewing the centre of weight change.

Figure 10 shows how in addition to the furnace roof, the superheater hanger rods also support the superheater headers. In an ideal case, the weight of the superheater is borne in its entirety by the hanger rods, but inequal stress distribution of the hanger rods might cause some of

the load to “escape” through the header or roof connection seen in the figure and thus not be seen by the ash weight measuring system.

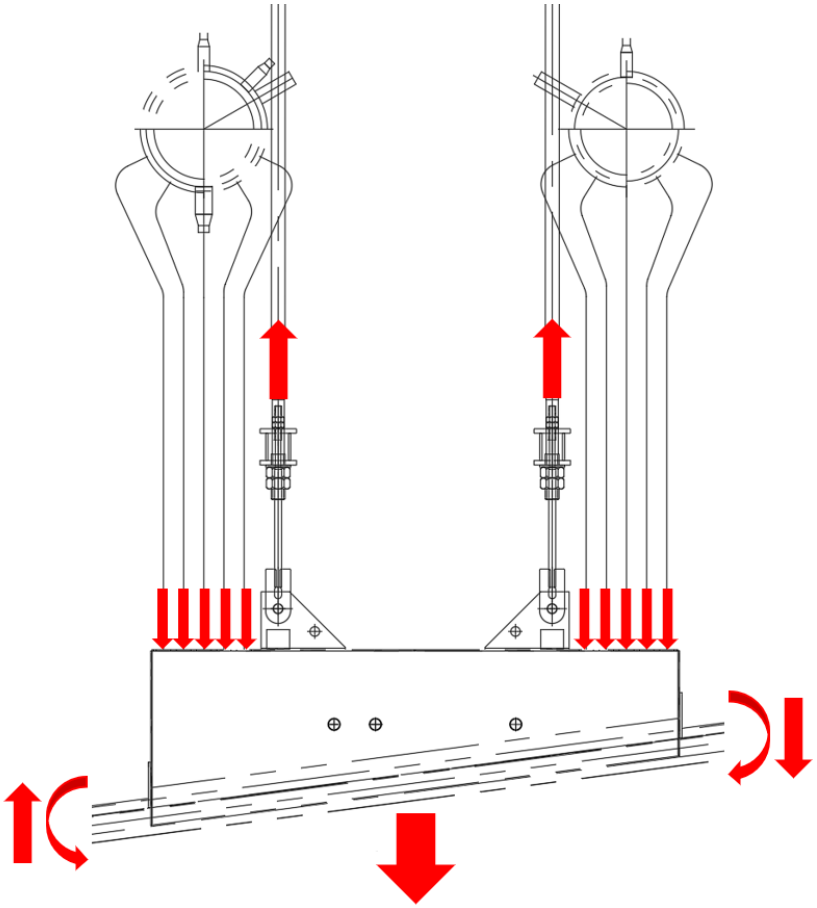

Figure 10. Static indeterminacy caused by inlet and outlet header and furnace roof.

Figure 11 shows how the riser pipes are supported by beams connected to the hanger rods. The beams connect the hanger rods together, allowing load pathing of adjacent rod loads through them and also along the risers themselves.

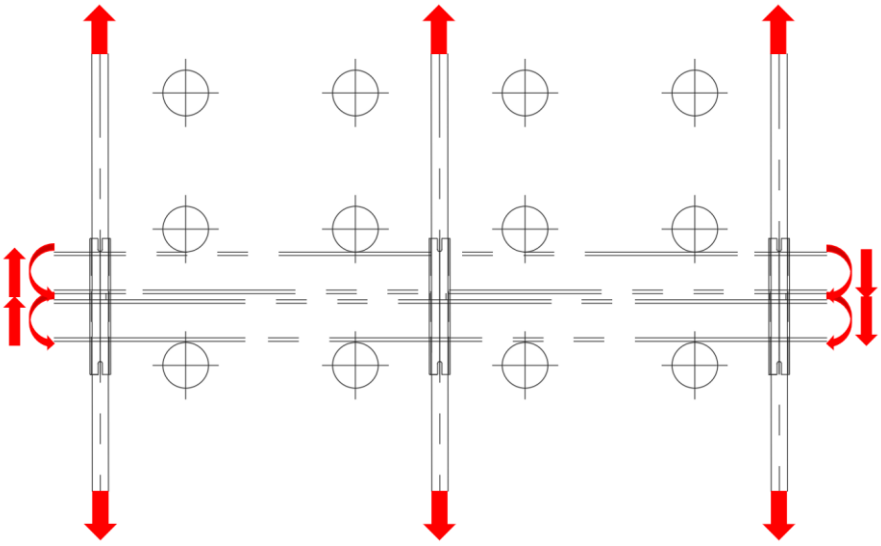

Figure 11. Static indeterminacy caused by riser support beams being connected to the hanger rods.

The magnitudes of the different types of static indeterminacy explained in this chapter need to be obtained to determine whether changes are necessary and where they should be made to improve the accuracy of ash weight measurements, however due to the static indeterminacy, obtaining analytical solutions is exceedingly challenging. Thus, the magnitudes will be analysed numerically using the finite element method.

4 Analysis methods

Based on reviewing literature around the loosening phenomenon of bolted joints, comparing it to Andritz's application, and looking at the static indeterminacy of the currently in use structure, it is concluded that the following analyses should be conducted to find effective means for improving the construction:

- Numerical analysis of the static indeterminacy caused by stress redistribution through the furnace roof, intermediate beam, riser supports, and headers so it is understood how an increase in the weight of a superheater element is distributed among the long hanger rods.
    - Based on the analysis, whether the vertical translation constraint between furnace roof and superheater support box need to be eliminated, and the superheater element's mass being only carried via the hanger rod to obtain the location of ash deposits more accurately is determined.
- Numerical analysis of stress redistribution dependence on tightening sequence of the hanger rods, distance between supports, and stiffness of the beam structure to find if the structure would benefit from simultaneous tightening of multiple rods by for example hydraulic tensioning.
- Sensitivity analysis of stress distribution's dependence on unevenness of temperature inside the penthouse to determine if broader measurements of the temperature variance are needed to assess the real-life condition in the penthouse, and if mixing the air inside the penthouse could used to achieve more uniform stress distribution of the hanger rods.

This section reports the steps taken and methods used for the analyses.

4.1 Static indeterminacy analysis

The static indeterminacy analysis consists of a model, where a single superheater stage of a recovery boiler is made and simulated to see how load pathing occurs through the various ways mentioned in Section 3 .

A superheater section of eight hanger rods is modelled based upon the design of a large capacity Andritz recovery boiler. Dimensions of the applied cross-sections are shown in Appendix 1. The shape and dimensions used for the model are shown in Appendix 2. The length of the hanger rods is 12000 mm.

Line body elements are used for the rods, pipes, and beams. Furnace roof and support boxes are modelled using plate element simplification where the plate dimensions are set to produce the same stiffness as the real structure. This is done so that the support box can be modelled with only one plate and to avoid having to model the furnace roof using solid elements, thus significantly saving computation time. The line and surface model of the structure is shown in Figure 12.

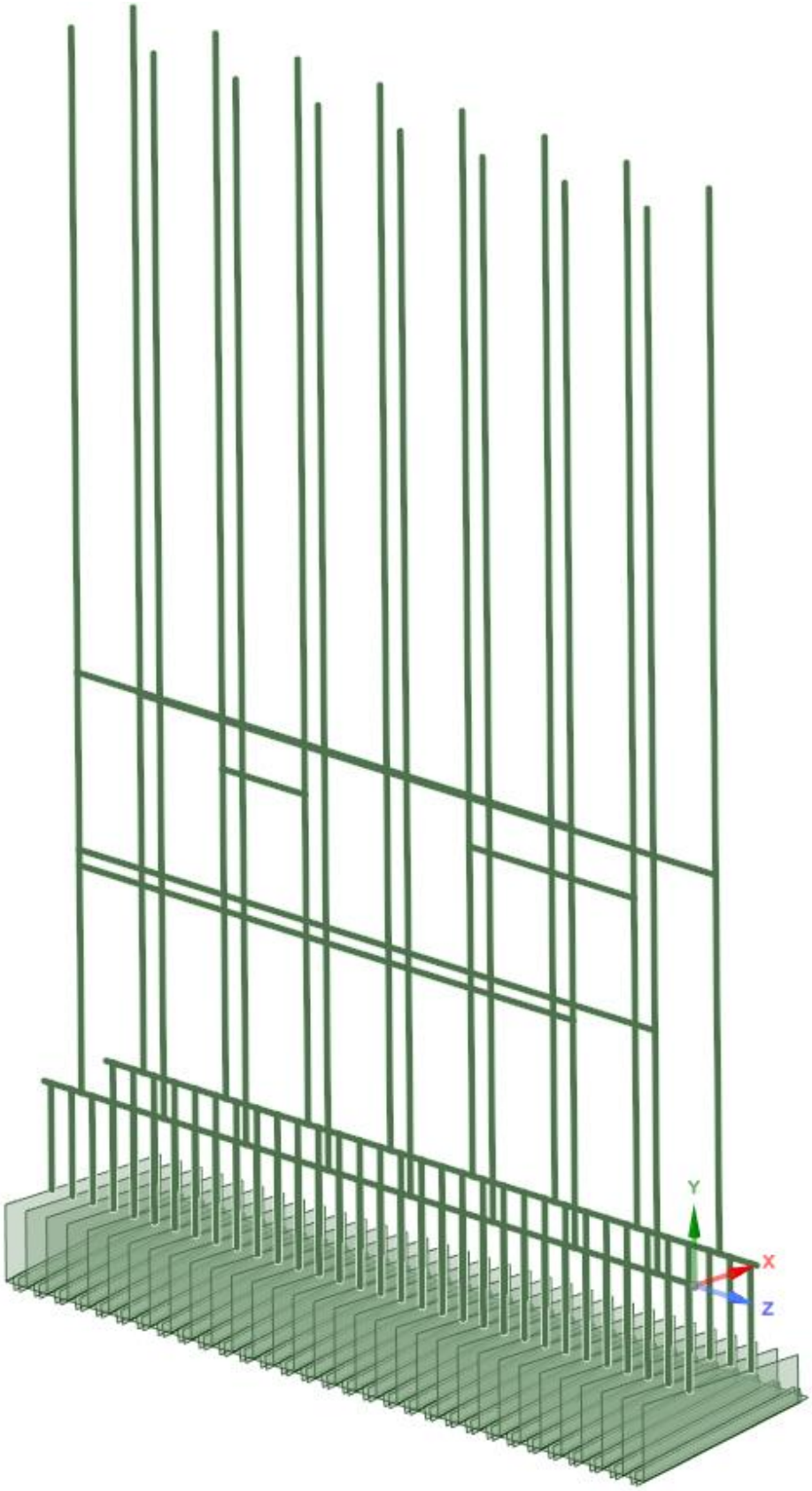

Figure 12. Static indeterminacy analysis line & surface model (headers suppressed for better visibility).

Parts in the model are connected using joints. Fixed joints are used for the connection between:

- Hanger rod–intermediate beam
- Intermediate beam–Superheater hanger rod (SH rod)
- Riser support beam–hanger rod
- Support box–furnace roof
- Inlet & outlet header–inlet & outer header piping
- Inlet & outlet header pipes–support box

General joints are used for the SH rod–support box connection where other degrees of freedom are fixed but rotation around the Z-axis is free.

The model is tested with a coarse (4000 mm max element size) and a fine (10 mm max element size) mesh for mesh sensitivity. The coarse mesh model is found to be significantly faster to analyze while the results obtained from the fine mesh model differ only slightly, which is why the coarse mesh is used for the remainder of the analyses. Linear elements are used, the mesh is presented in Figure 13, Figure 14 & Figure 15.

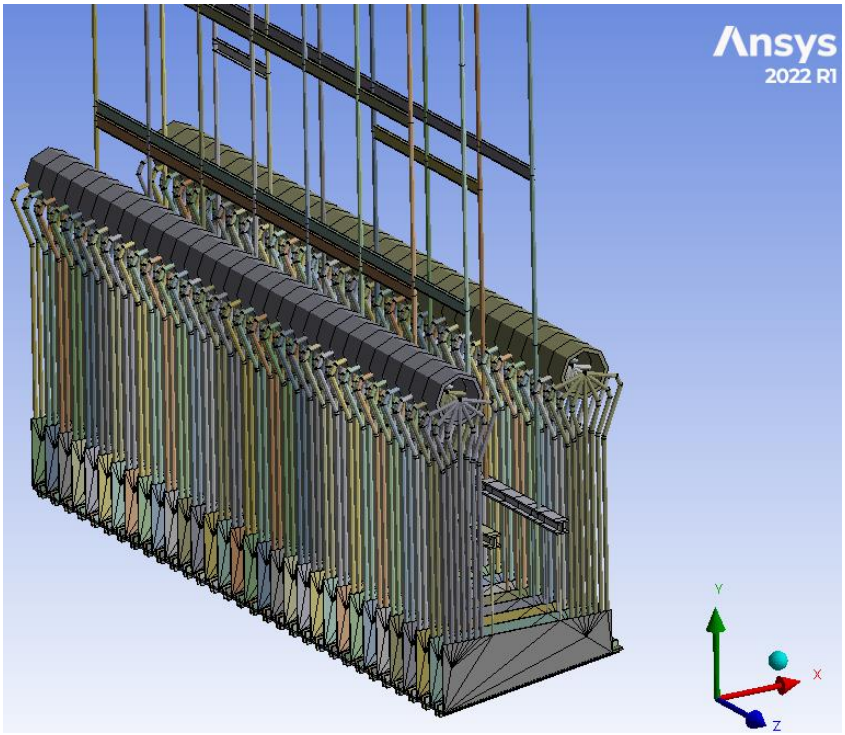

Figure 13. Static indeterminacy analysis mesh isometric view.

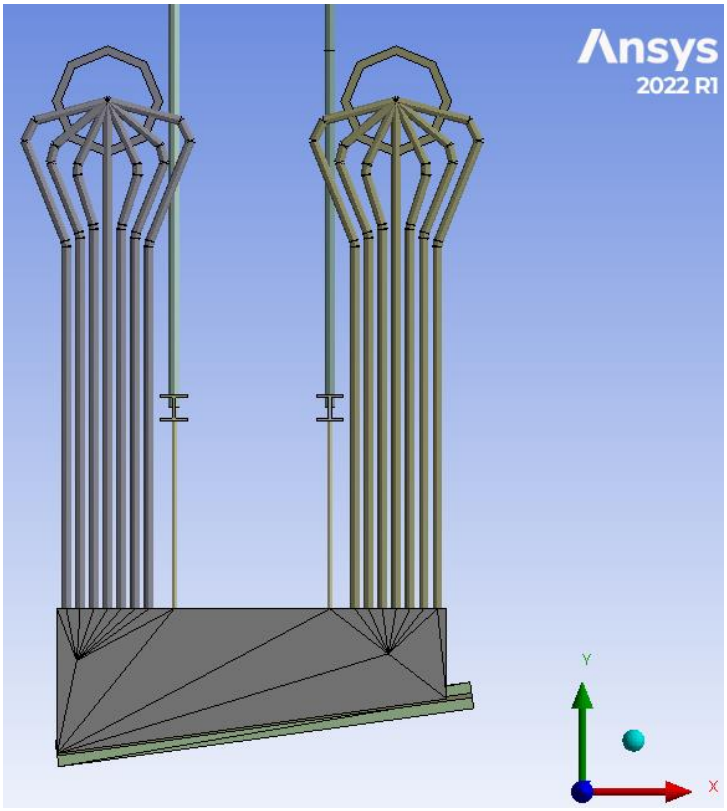

Figure 14. Static indeterminacy analysis mesh right hand side view.

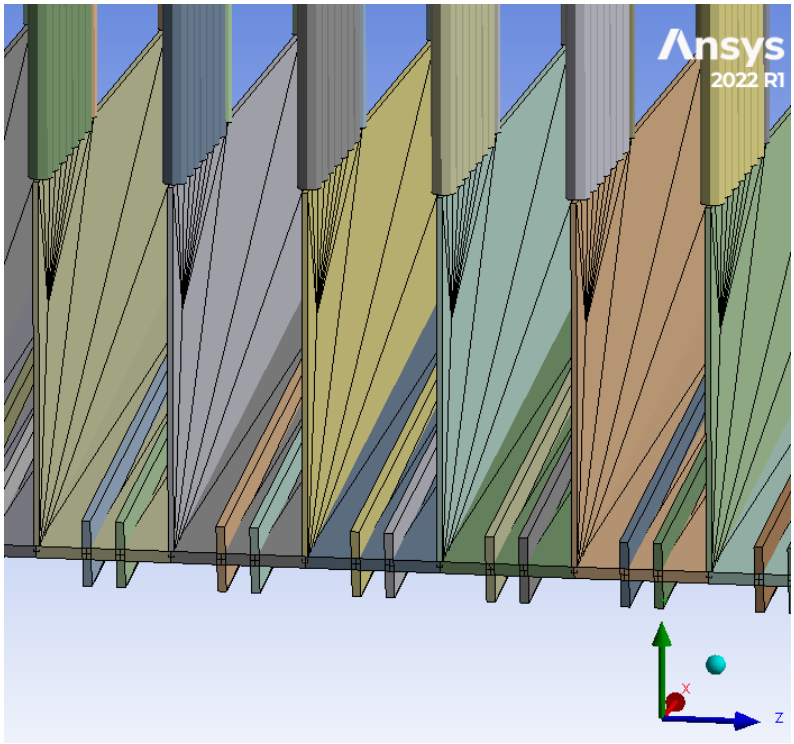

Figure 15. Static indeterminacy analysis furnace roof and support box meshing.

Material is steel with density ρ = 7850 kg/m^3, Poisson's ratio v = 0.3, and Young's modulus E = 170 GPa (At 360 °C, see Figure 4). A linear elastic material model is used. Three different load cases are used to conduct the analysis, with all loads applied in the negative Y-direction. Load case 1 (Figure 16) consists of loads applied on the bottom edges of the support boxes. A load of 57.5 kN on each support box is used to represent the weight of the superheater element piping below the furnace roof, the geometry of which is not modelled.

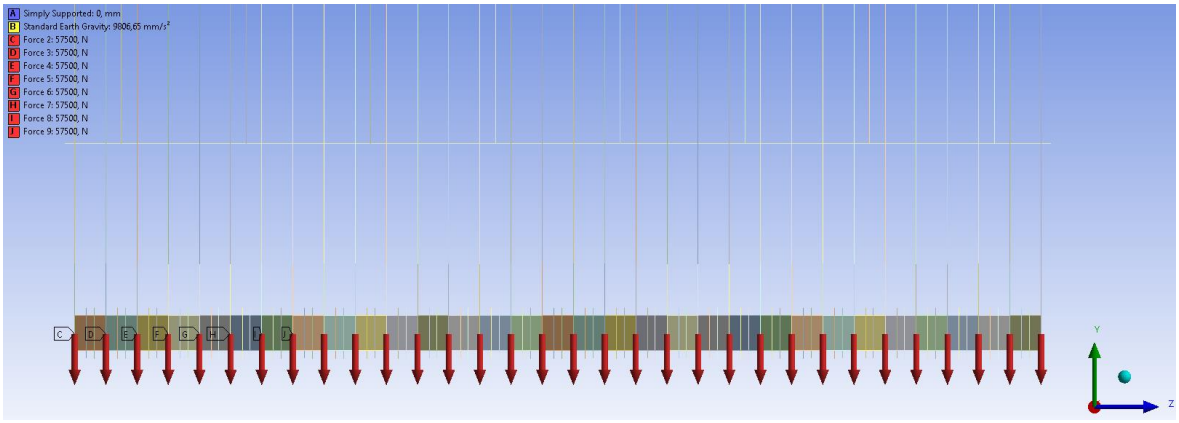

Figure 16. Static indeterminacy analysis load case 1.

Load case 2 (Figure 17) adds a single force of 1 kN applied on the bottom edge of the 22nd (numbered in the positive Z direction) support box in addition to the platen weights of load case 1 to simulate a concentrated ash weight.

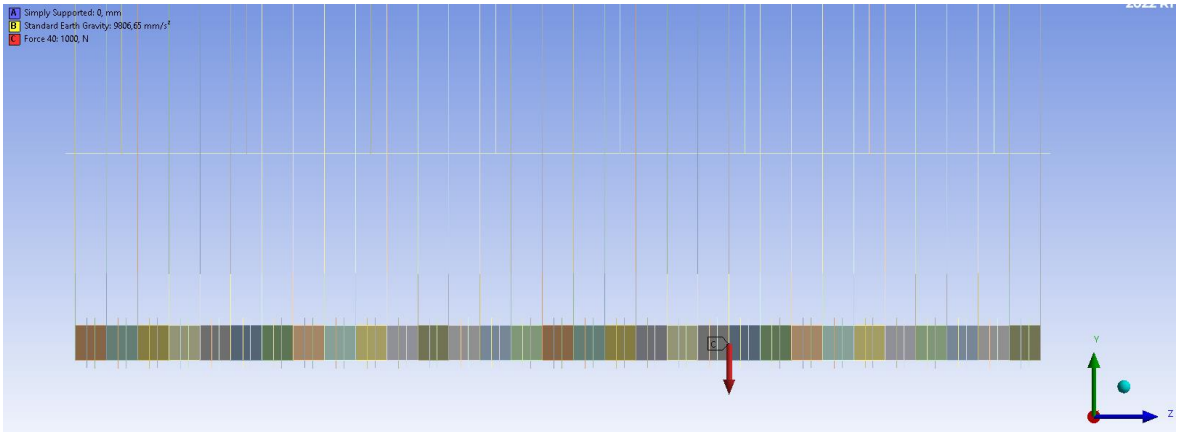

Figure 17. Static indeterminacy analysis load case 2.

Load case 3 (Figure 18) adds three 250 N and four 500 N forces applied on the bottom edge of the 5–7 and 20–23 support boxes respectively, in addition to the platen weights of load case 1 to simulate a distributed ash weight.

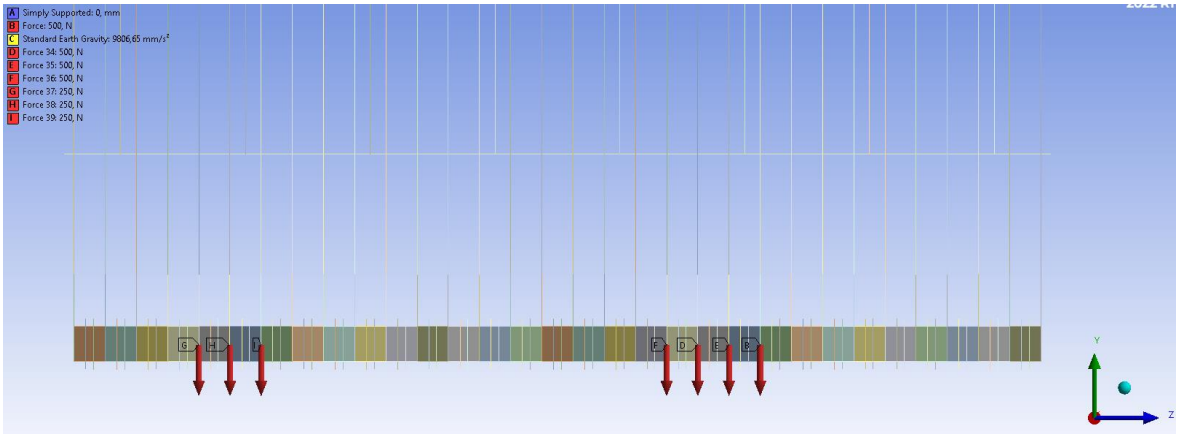

Figure 18. Static indeterminacy analysis load case 3.

In addition to the load cases, the structure is loaded by its own weight, for which Ansys standard earth gravity 9,806 m/s^2 is used. The structure is constrained with simple supports that are applied on the top ends of the hanger rods. They are presented in Figure 19.

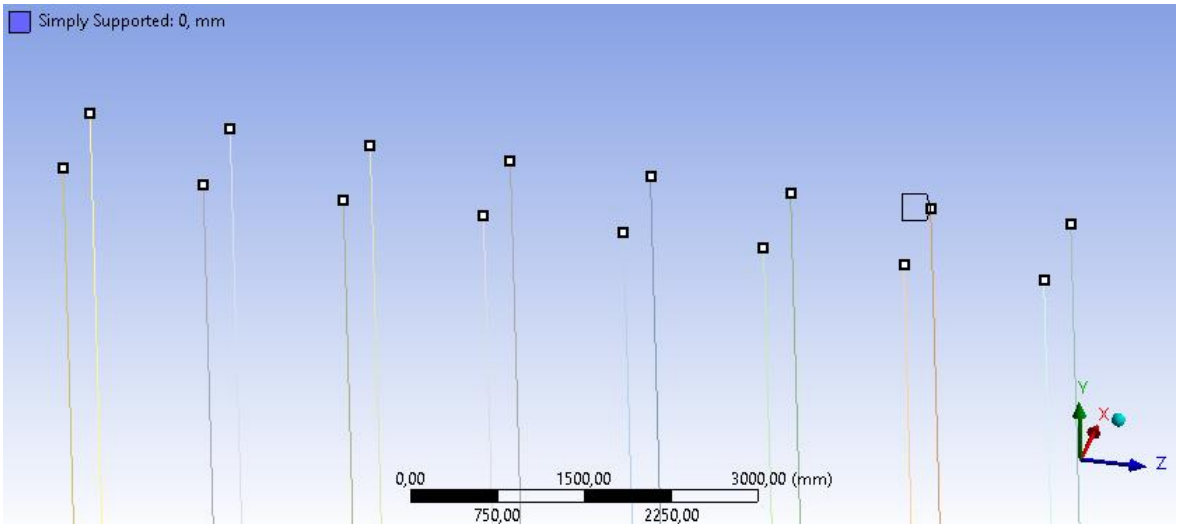

Figure 19. Static indeterminacy analysis simply supported boundary conditions.

Geometrically nonlinear analysis is used so that the deflections of the different parts affect the load pathing. When analysed, the model deformations seem to stabilize between the first and second time step, which is why the total number of steps in the analysis is set to 2. Equivalent (von-Mises) stresses are measured from the top ends of the hanger rods. Stress

values of load case 1 are subtracted from values obtained from load case 2 and 3 to get the stress change values. These are then graphed for the rod number from 1 to 8. The process is repeated as changes are made to the model to see how the stress change values are affected. Sectioned intermediate beam refers to a change in the model where the intermediate beams of both the front and rear hanger rods are divided into sections that rods 1&2, 3&4, 5&6, and 7&8 support separately.

4.2 Tightening sequence analysis

This section reports on the tightening sequence analysis, where the model used in the static indeterminacy analysis is extended from 8 to 19 total hanger rods, from 32 to 76 total SH rods, and simulated to see how rod tension is affected by the tightening sequence. An optimal tightening sequence and preload values are obtained.

The analysis' line & surface model is shown in Figure 20, the main difference compared to the static indeterminacy analysis model being that the superheater is longer, therefore having more hanger rods, and them being suspended from the boiler beam structure (tertiary, secondary, and primary beams). Dimensions of the applied cross-sections are shown in Appendix 1. The riser supports' vertical distance from the intermediate beams and the side view dimensions of the model are the same as in the static indeterminacy analysis (See Appendix 2). How the riser supports and intermediate beams connect to the hanger rods can be seen in Figure 21 and Figure 22. The length of the hanger rods is 12000 mm. The lengths of the three intermediate beam sections are 7376 mm, 8624 mm, and 7376 mm in the positive Z-direction. The distance of outermost hanger rods on each intermediate beam is 568 mm from the edge. For outermost SH rods the distance is 100 mm.

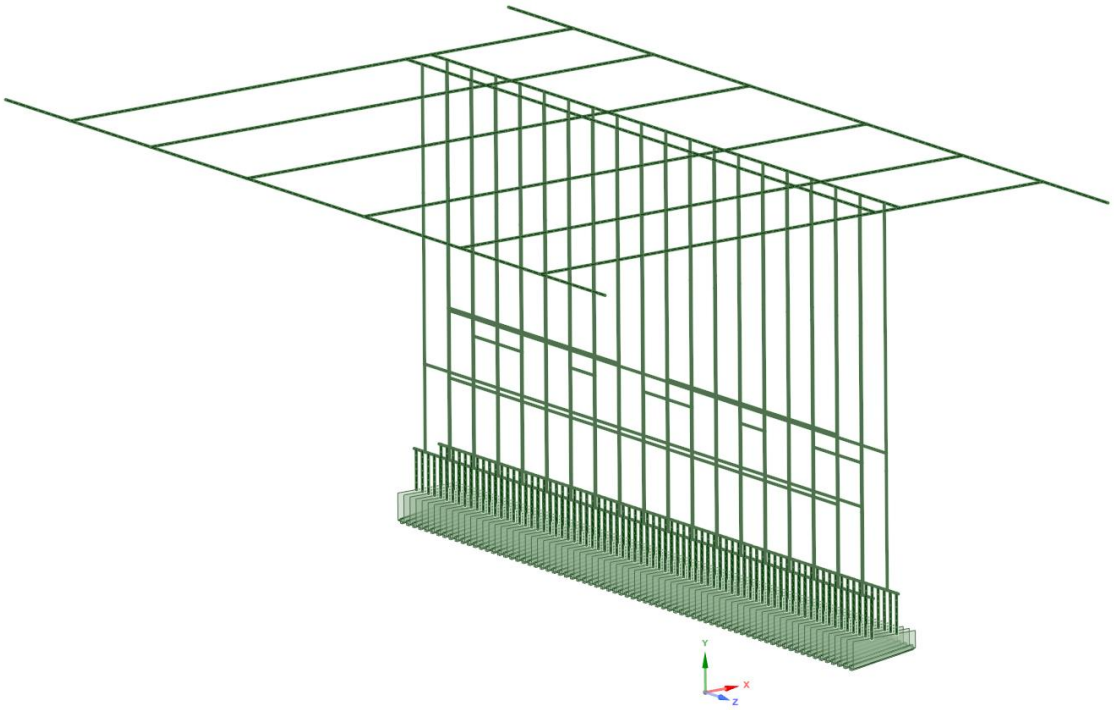

Figure 20. Tightening sequence analysis line & surface model (headers suppressed for better visibility).

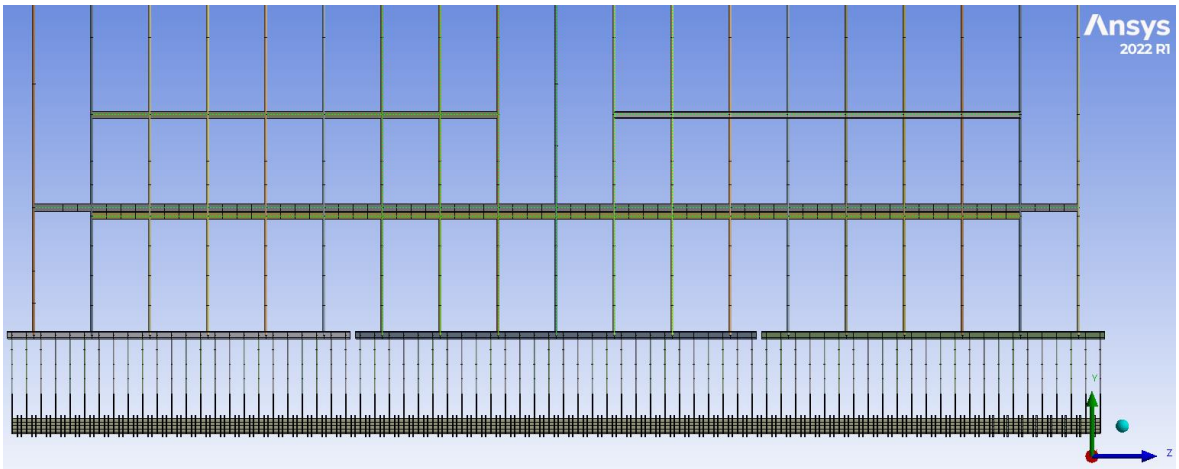

Figure 21. Tightening sequence analysis front rod riser supports.

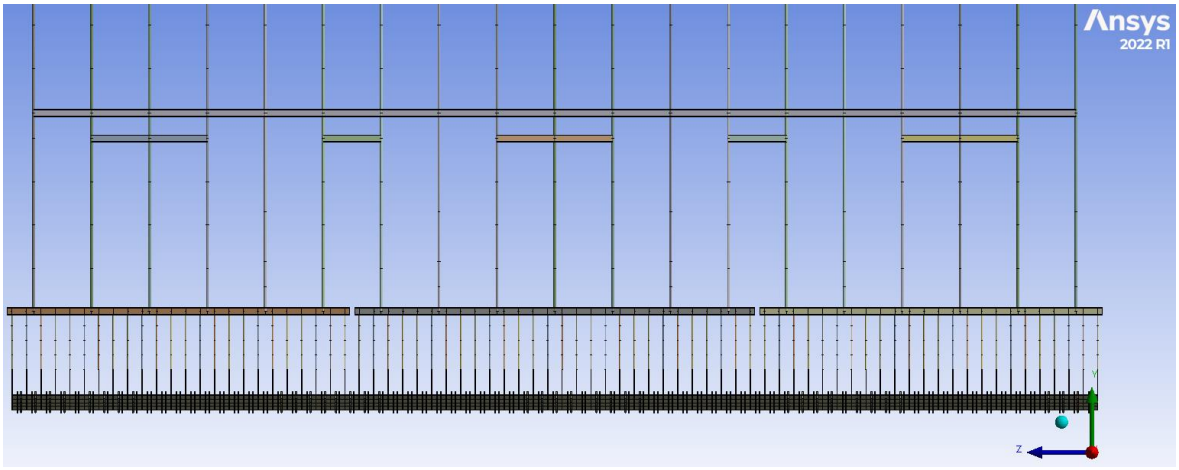

Figure 22. Tightening sequence analysis rear rod riser supports.

Parts in the model are connected together using joints. Fixed joints are used for the connection between:

- Primary beam-secondary beam
- Tertiary beam-hanger rod
- Hanger rod–intermediate beam
- Intermediate beam–SH rod
- Riser support beam–hanger rod
- Support box–furnace roof
- Inlet & outlet header–inlet & outer header piping
- Inlet & outlet header pipes–support box

General joints are used for the SH rod–support box connection where other degrees of freedom are fixed but rotation around the Z-axis is free. General joints with free rotation around the X-axis are used for the secondary beam-tertiary beam connections.

Similar mesh to the static indeterminacy analysis is used, with the addition of the boiler beam structure shown in Figure 23. The mesh has additional nodes at locations where boiler beam loads are applied to achieve realistic beam deflections (see Appendix 3).

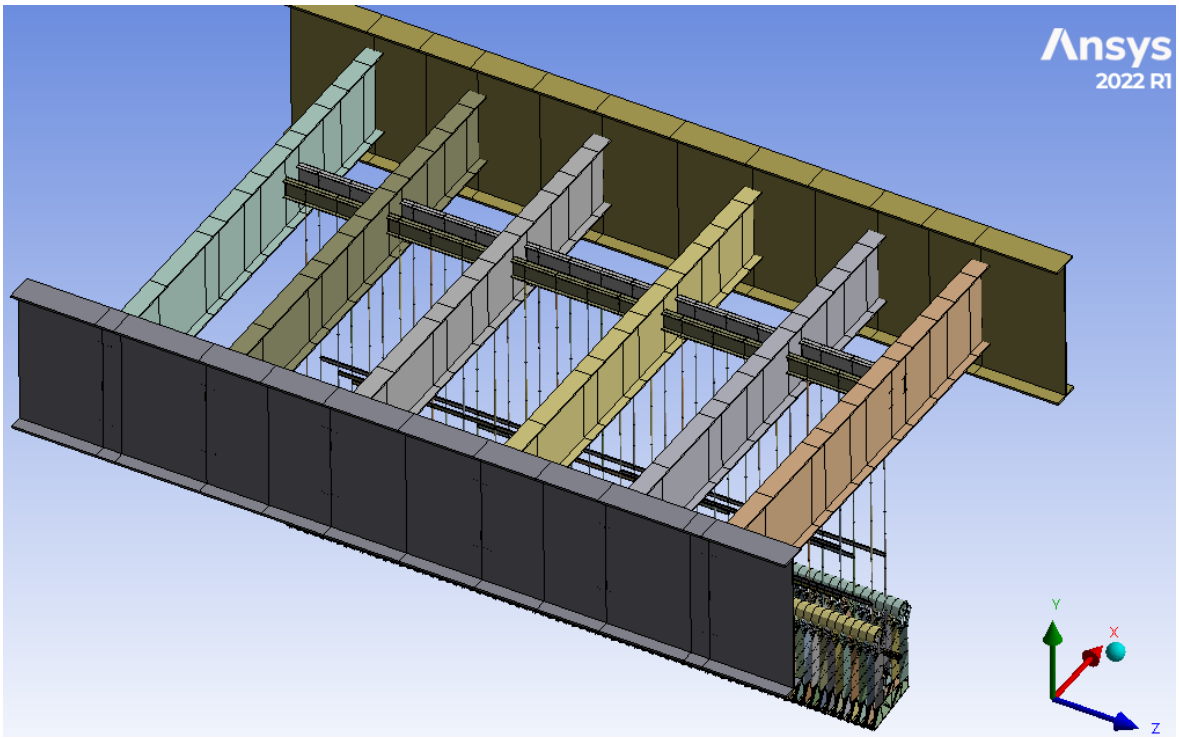

Figure 23. Tightening sequence analysis boiler beam mesh.

Material is steel with density ρ = 7850 kg/m3, Poisson's ratio v = 0.3, and Young's modulus E = 200 GPa (room temperature). A linear elastic material model is used. The load case consists of loads applied on the bottom edges of the support boxes. A load of 57.5 kN on each support box (76 in total) is used to represent the weight of the superheater element piping below the furnace roof, the geometry of which is not modelled (See Figure 16). Additionally, the boiler beams are loaded to represent the weights of the other superheaters, steam drum, side and front walls. This is shown in Appendix 3. The structure is loaded by its own weight, for which Ansys standard earth gravity 9,806 m/s^2 is used. All loads are applied in the negative Y-direction. The structure is constrained with simple supports at end of the primary beams, the rotation of which around the Z-axis is also constrained. The boundary conditions are shown in Figure 24. When compared against boiler beam deflection

calculations done by Andritz, the applied boundary conditions and loads are confirmed as being realistic.

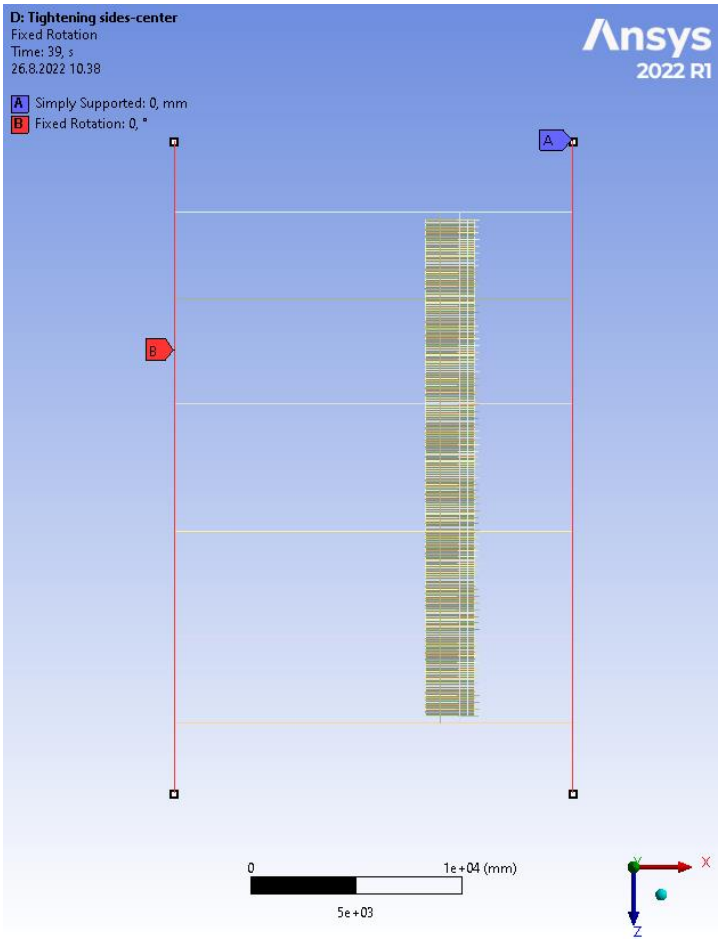

Figure 24. Tightening sequence analysis boundary conditions.

An equally distributed rod axial force is the average of the initial load distribution. This average is used as the first tightening sequence iteration's pretension value. Tightening is controlled via bolt pretension objects applied to each rod. After the sequence is simulated, a new hanger rod load distribution is obtained. By comparing it to the average, each hanger rod's pretension value is adjusted. The iteration is repeated until a low enough variance in tension condition is obtained.

The long hanger rods' tightening is simulated first. After that, the SH rods' tightening sequence is evaluated to see how a low variance in pretension can be obtained and how tightening them affects the previously tightened long hanger rods. A sequence from the centre to the sides is iterated first. It is found to cause too high preload requirements for a single pass tightening, therefore a sequence from sides to the centre is iterated. The sequences used are shown in Appendix 4.

The load distribution of both the hanger rods and SH rods is obtained pre- and post-tightening. The variance in load distribution of each iteration is calculated by comparing the maximum and minimum load values to the average.

4.3 Temperature effect analysis

The temperature effect analysis examines how the load distribution in the structure changes after tightening in response to an increase in penthouse temperature as the boiler starts up. The sensitivity of the load distribution to the temperature distribution is analysed. Creep is not considered as the model does not account for local stresses accurately. Also due to lack of prior research done on the creep behaviour of different steels, obtaining the creep constants of the hanger rod materials which would be required for the creep analysis is not possible within the scope of this study.

The model is identical to the tightening sequence analysis model, including identical loads and boundary conditions with exceptions mentioned in this chapter. Young's modulus is reduced to E = 170 GPa (at 360 °C, see Figure 4) due to the elevated temperature for all parts, except the boiler beams which have E = 200 GPa as they are outside the insulation layer. The coefficient of thermal expansion used is α = 1.2E-05.

$$T = 360 - az^2 \quad (4)$$

A made-up temperature distribution along the Z-axis for the rest of the structure is modelled with Ansys thermal conditions using Equation (4), where *a* is a scalar for the temperature variance and *z* is the distance from the centre of the structure along the z-axis. Table 2 lists the temperature ranges for different *a* values.

Table 2. Range of the temperature distribution in the structure for different a values.

a	Temperature range [°C]
5E-08	7
1E-07	14
2E-07	28
3E-07	41

The headers and their connecting piping experience higher temperatures in real world applications due to steam temperature inside them. Case 2 where the headers and their connecting piping experience 500 °C temperature is analyzed separately to see whether this effect is considerable. The case reduces the Young's modulus of the headers and connecting piping further to E = 158 GPa (see Figure 4).

The temperature distribution in the structure when a = 3E-07 is shown in Figure 25 (Case 1).

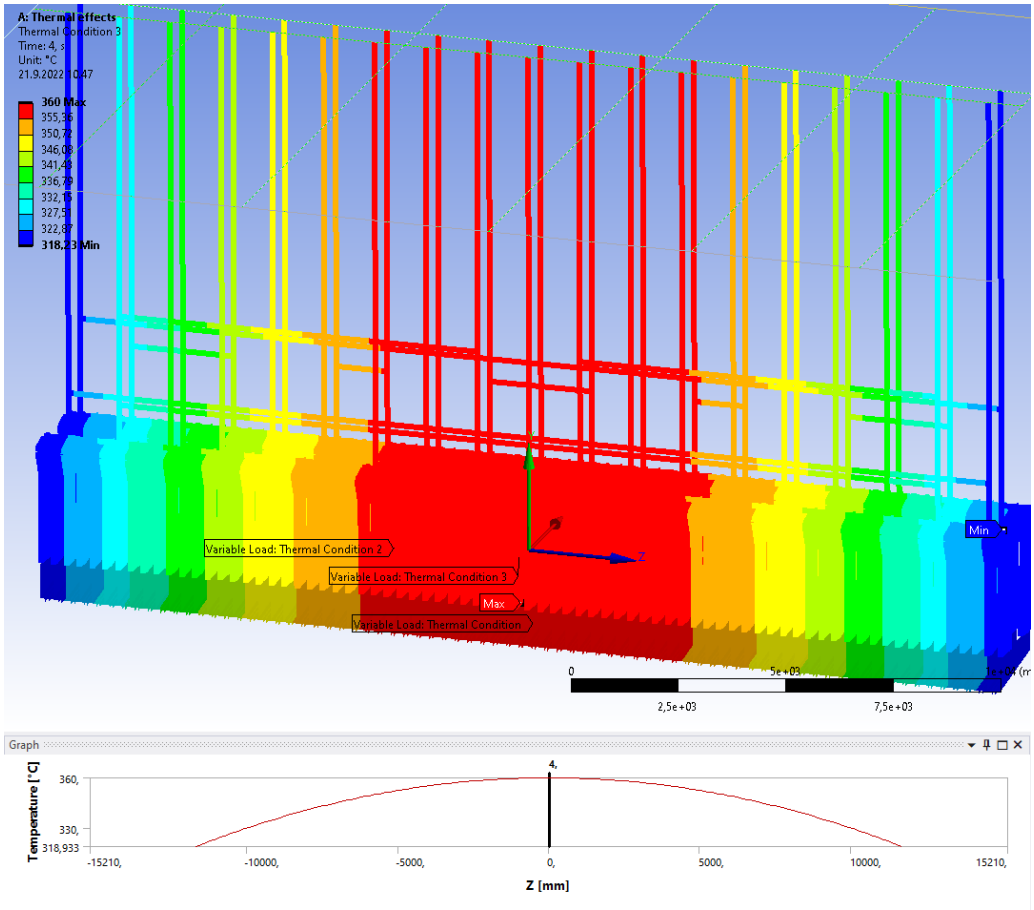

Figure 25. Temperature distribution when a = 3E-07 (Case 1).

Similarly to the tightening sequence analysis, the resulting load distribution is obtained for each temperature distribution to see how sensitive the structure is to it.

5 Results

In this section, the results of each of the three analyses are listed and examined.

5.1 Static indeterminacy analysis

Mesh sensitivity analysis results on the front and rear rods is presented in Figure 26. Both the front and rear rods' stresses were analysed, and although differences are found in the absolute stress values between them, the stress change values are found to be very similar. Therefore, the rest of the results only show the stress change values of the front rods.

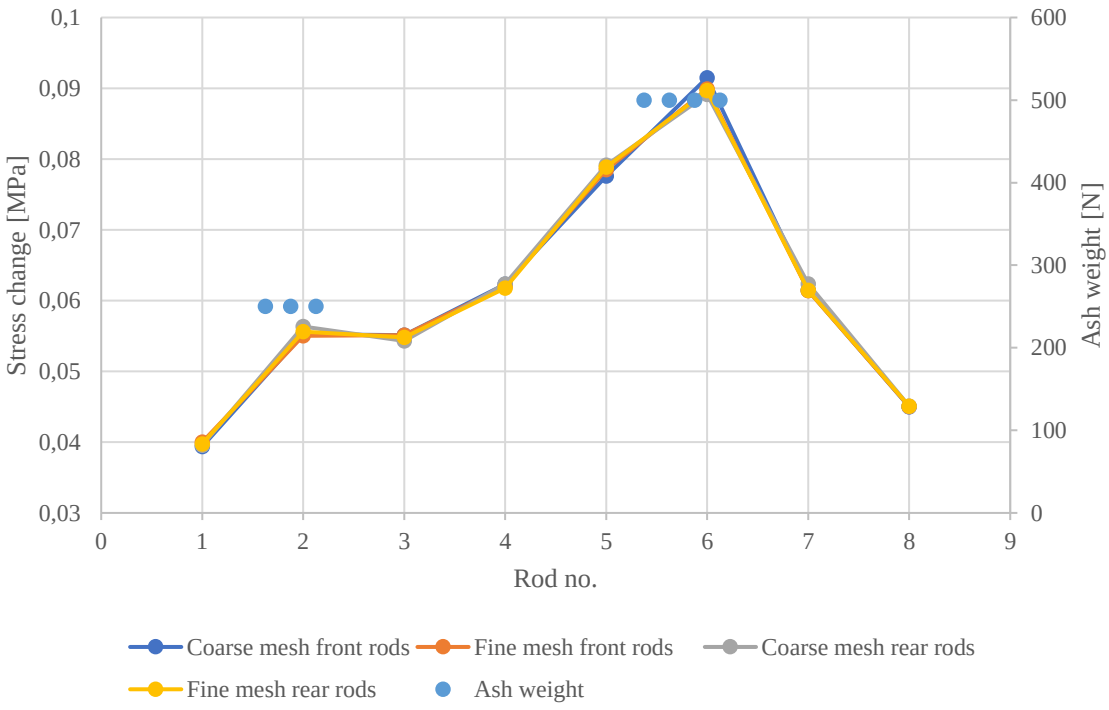

Figure 26. Static indeterminacy analysis comparison between coarse and fine mesh on front and rear rods.

Figure 27 shows how the concentrated ash weight affects the hanger rod stresses and Figure 28 how the distributed ash weight affects the rods.

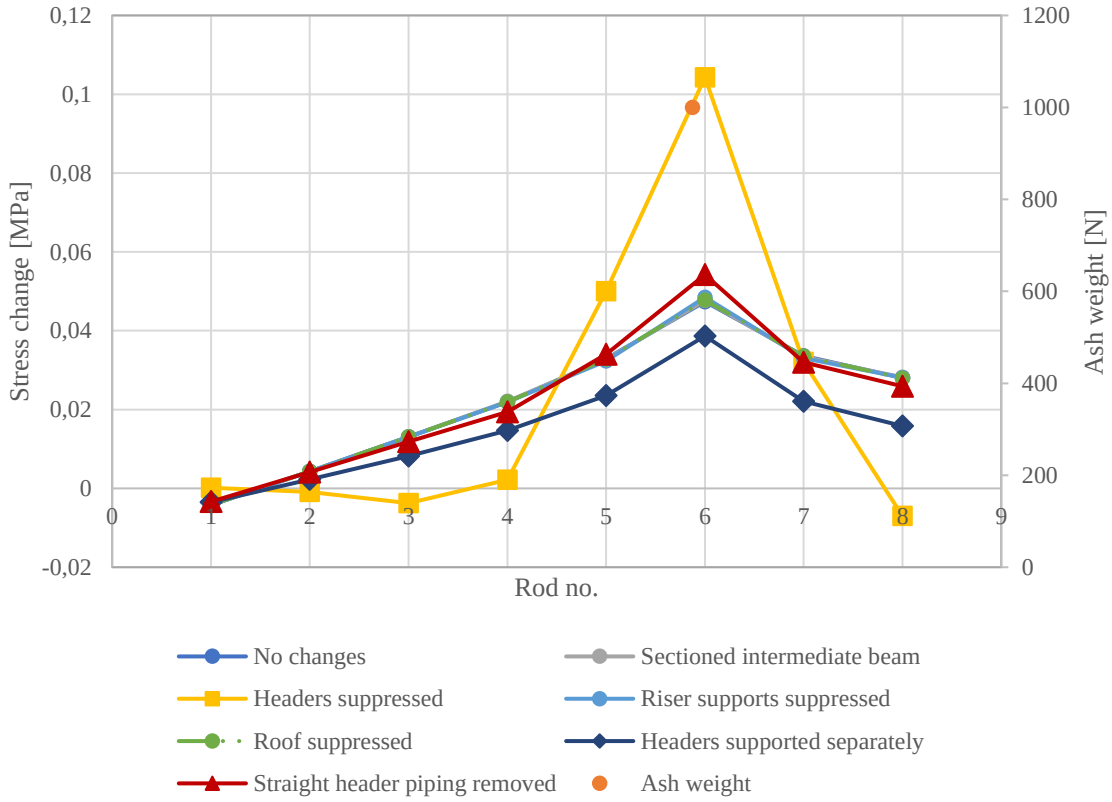

Figure 27. Static indeterminacy analysis front rod concentrated ash weight stress change.

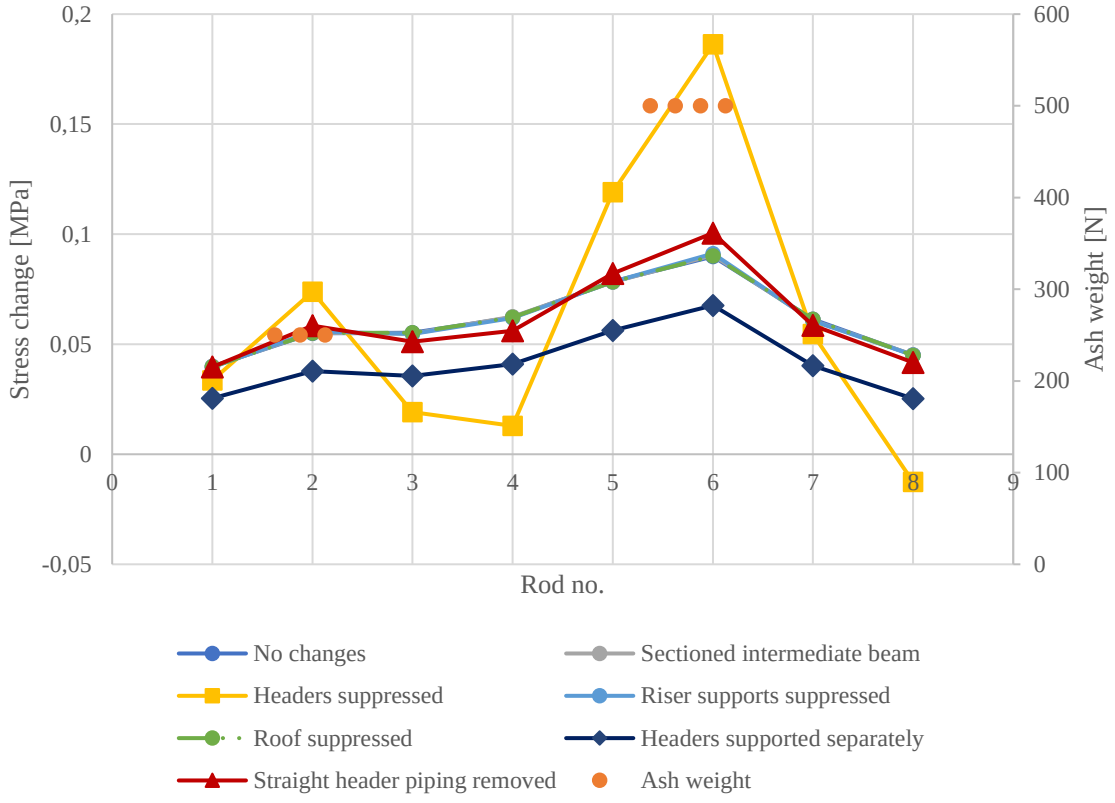

Figure 28. Static indeterminacy analysis front rod distributed ash weight stress change.

Based on the figures, the headers seem to cause most of the load pathing, preventing any benefit from changes made to the model elsewhere. Removing the unbent piping connected to the headers reduces the stiffness, thus increasing accuracy slightly. Supporting the headers separately only causes the weight of the entire model to redistribute among the pre-existing and new supports. Thus, the stress values are reanalysed, this time having the headers suppressed from the model while the same changes are made to the model cumulatively to see what kind of improvements in accuracy can be obtained. The resulting stress changes are shown in Figure 29 and Figure 30.

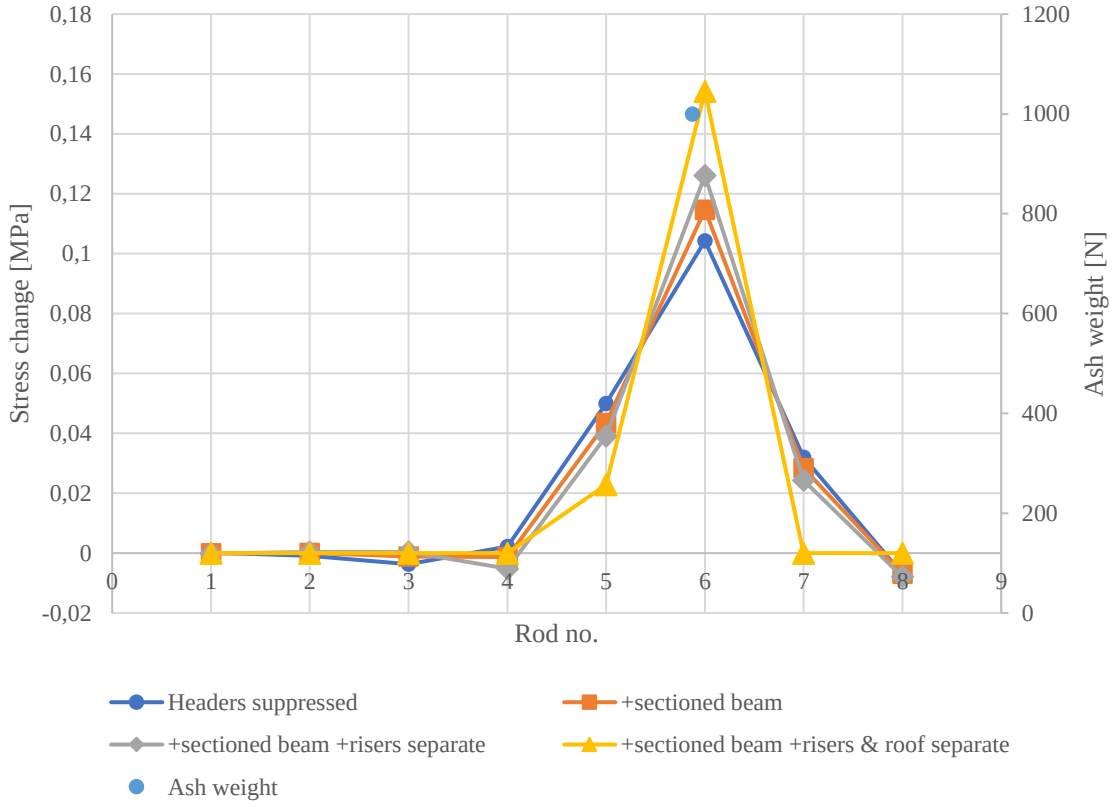

Figure 29. Static indeterminacy analysis front rod cumulative changes when headers are suppressed (concentrated ash weight).

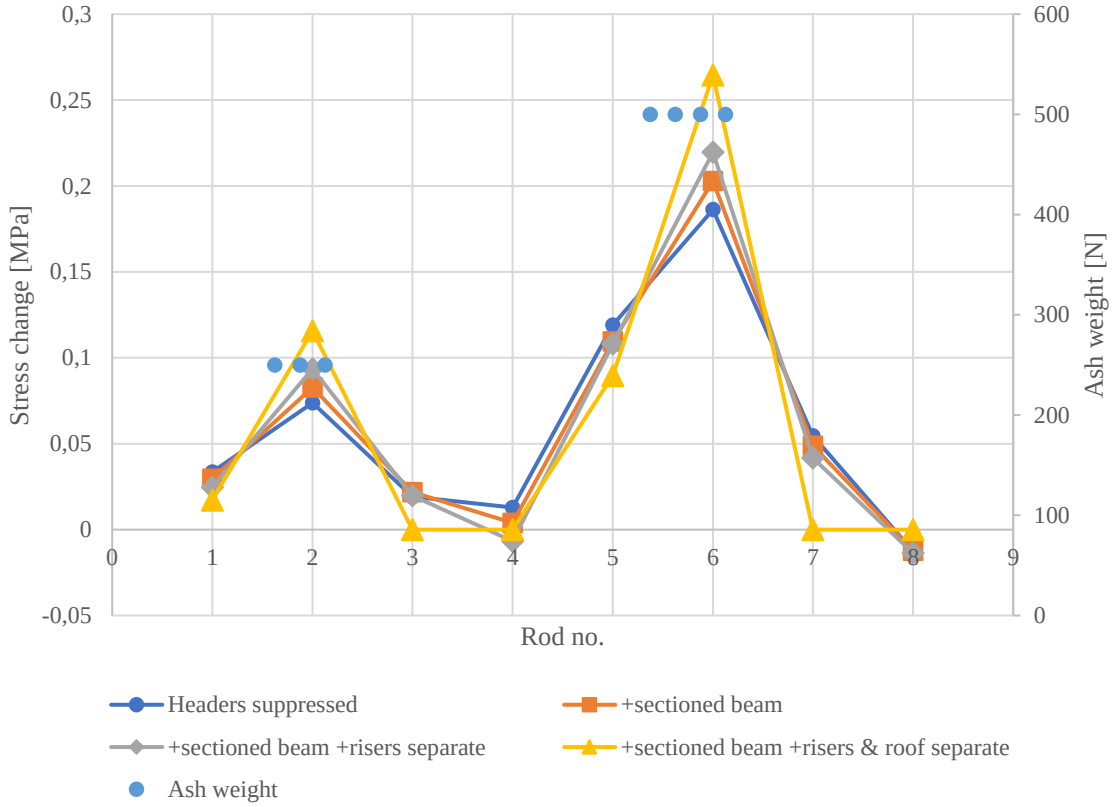

Figure 30. Static indeterminacy analysis front rod cumulative changes when headers are suppressed (distributed ash weight).

As can be seen from the figures, with the headers suppressed, the location of the ash weight can be obtained with increasing accuracy as cumulative changes are made.

The conclusion of the analysis is that making changes elsewhere (sectioned beam, roof connection etc.) does not improve accuracy meaningfully unless the load pathing resulting from the header stiffness is dealt with. It should be noted that the real-world application has multiple superheaters, each having different sized headers and varying amount of connecting piping. This affects load pathing and therefore the ash weight measurement accuracy of each of the superheaters. Also, the stress changes of the rods are very small, which makes measuring them accurately in real life conditions challenging.

5.2 Tightening sequence analysis

The initial load distribution in the structure is shown in Figure 31 for hanger rods, and Figure 32 for SH rods. The initial deformation of the hanger rod top-ends is shown in Figure 33.

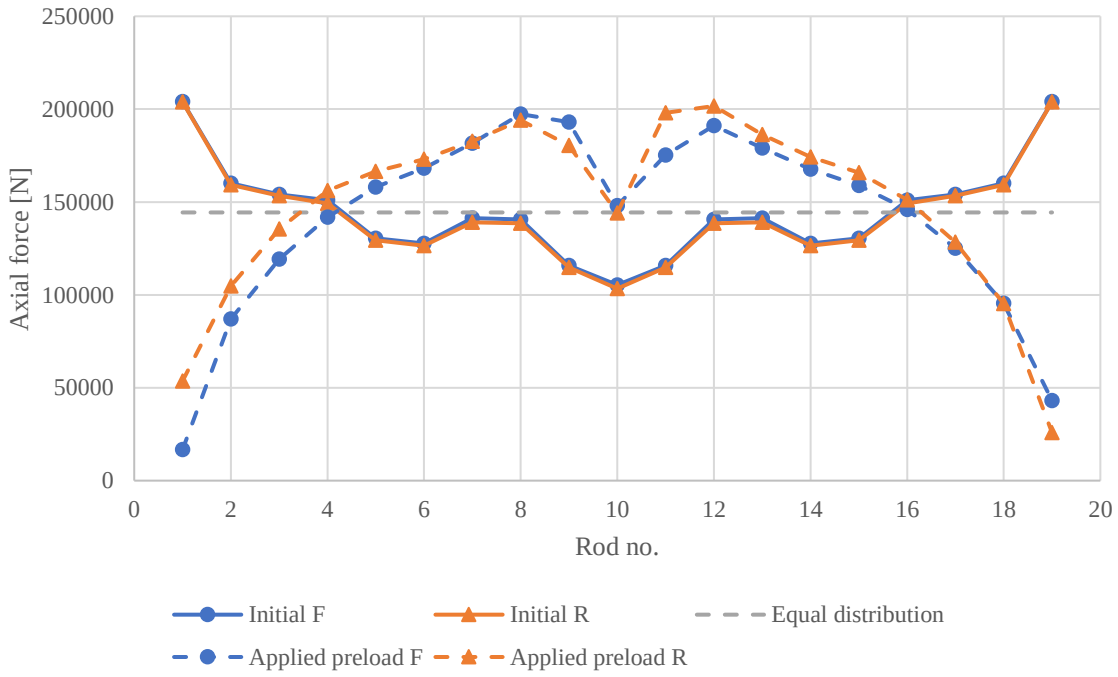

Figure 31. Initial load distribution of hanger rods.

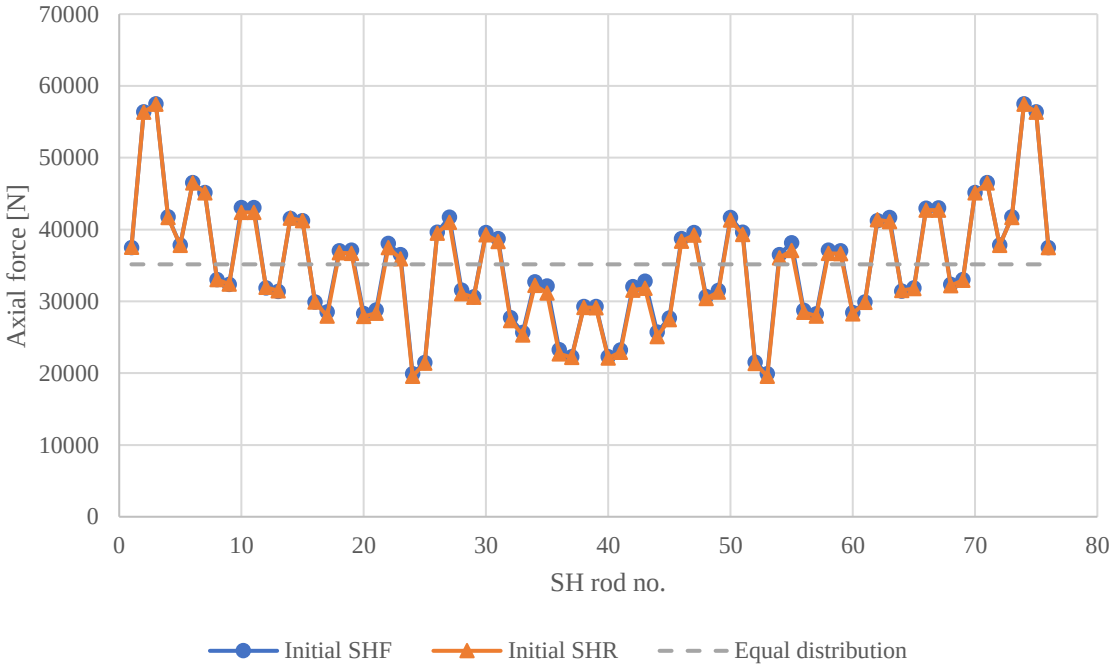

Figure 32. Initial load distribution of SH rods

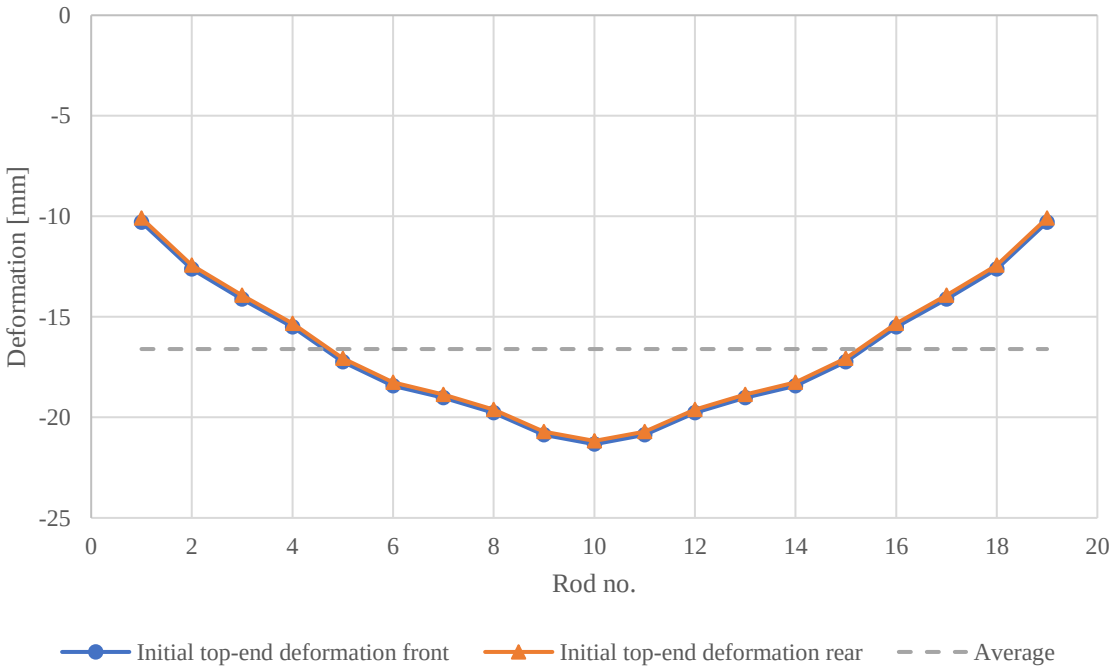

Figure 33. Initial deformation of hanger rod top-ends.

The initial load distribution of the hanger rods seems to generally follow the deformed shape of the structure, with differences arising from the intermediate beams having differing amount of deflection throughout their lengths. The SH rods distribution follows the hanger rods with the SH rods immediate to the hanger rods having higher preload than the more remote ones.

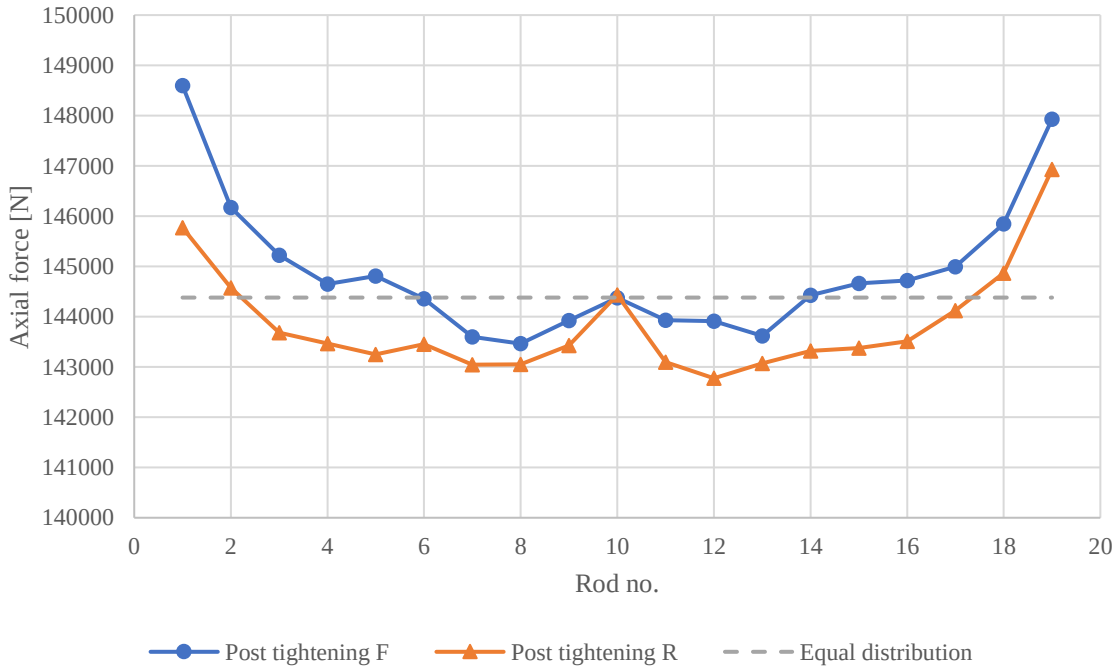

Figure 34. Post hanger rod tightening load distribution.

A relatively even distribution is obtained after the 5th iteration. Note the change in vertical axis range in the figure. Tightening in the hanger rods also brings the load distribution in the SH rods nearer to the equal distribution line. This SH rod distribution prior to tightening them is shown in Figure 35.

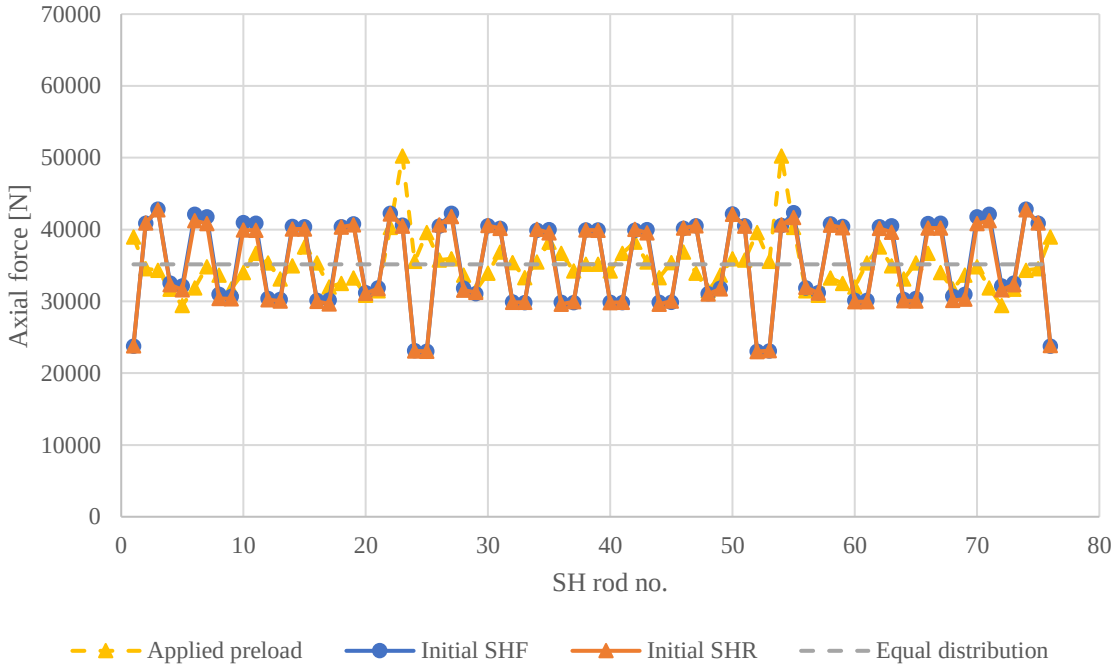

Figure 35. SH rod load distribution piror to SH rod tightening.

The SH rods nearest to the edges of the intermediate beams have noticeably lower preload. Figure 36 and Figure 37 show how tensioning the SH rods affect the load distribution

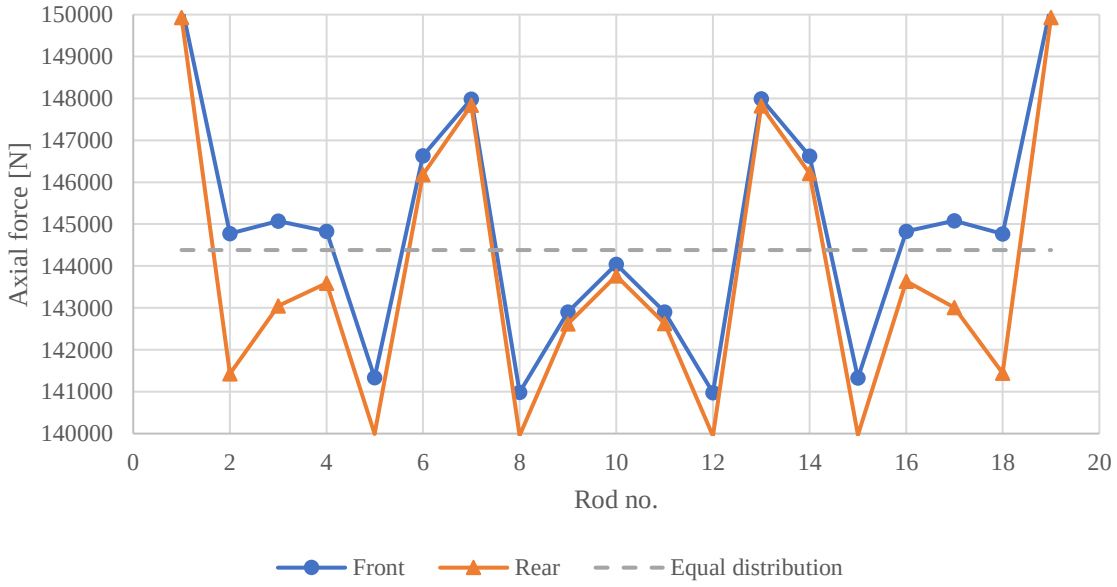

Figure 36. Post hanger rod and SH rod tightening load distribution.

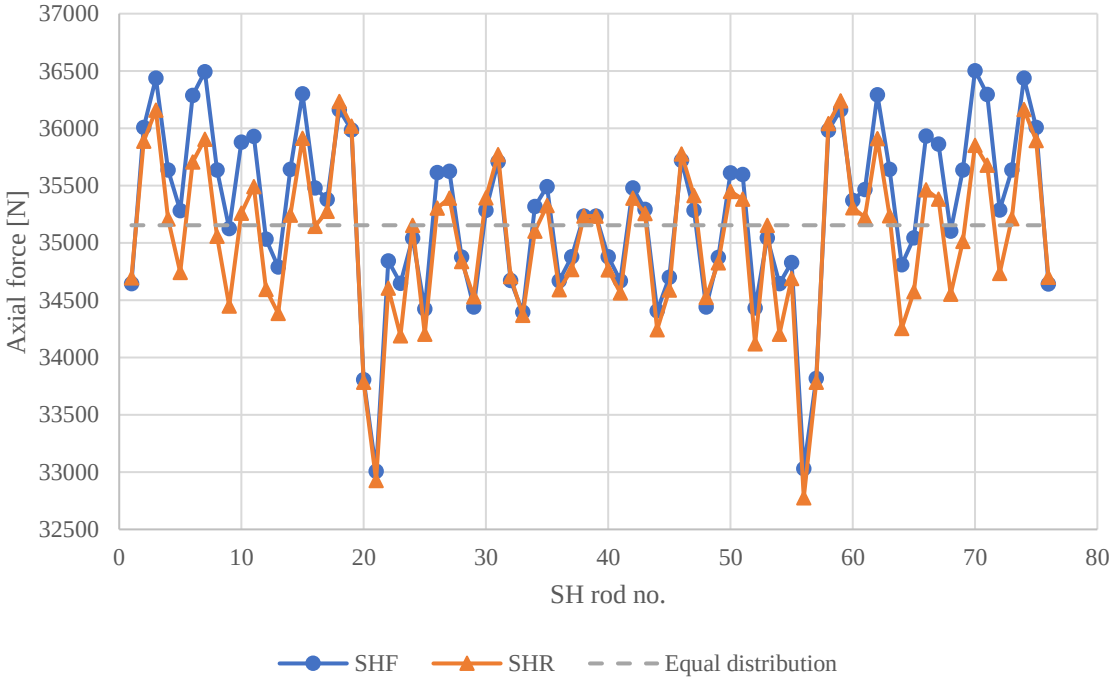

Figure 37. Post hanger rod and SH rod tightening load distribution of SH rods.

By the 3rd iteration the load distribution of the SH rods has been improved (note the change in vertical axis range), with the load distribution of the hanger rods worsening slightly. High deviance in axial force seems to occur on the outermost SH rods of the intermediate beams. Achieving uniform tension of these rods is noticed to be particularly difficult. Figure 38 and Figure 39 show how tightening the hanger rods affects the total deformation of the structure.

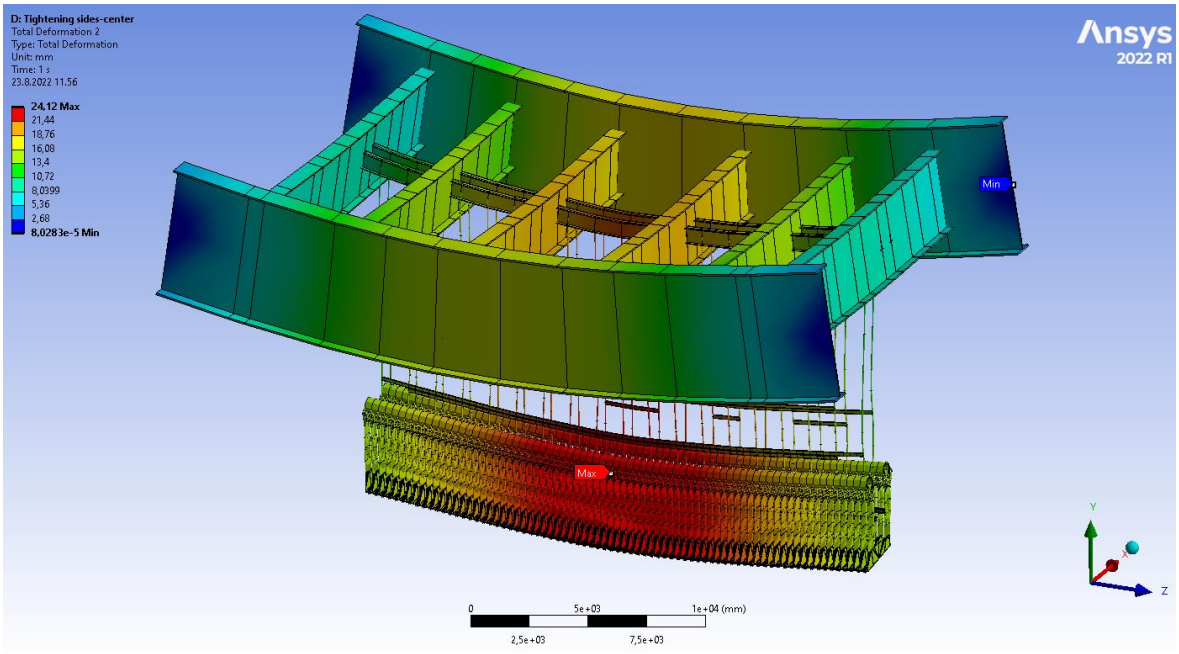

Figure 38. Tightening sequence analysis total deformation of model prior to tightening. (100x deformation scale)

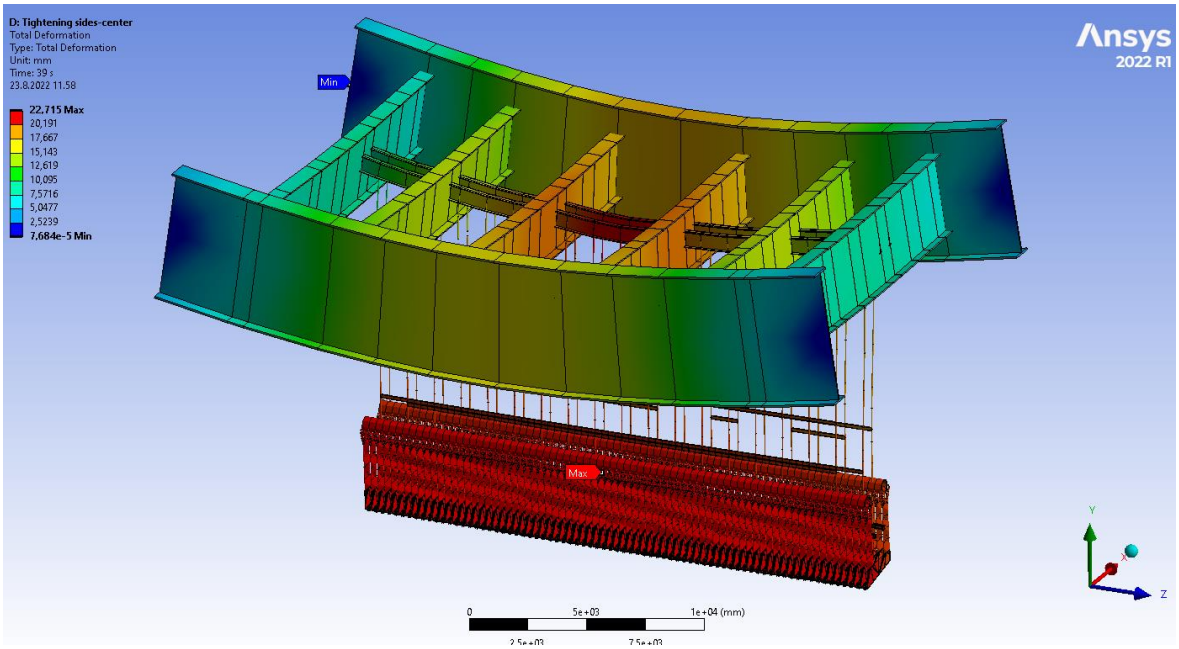

Figure 39. Tightening sequence analysis total deformation of model after tightening hanger rods. (100x deformation scale)

Figure 40 shows how the axial force changes in the front 1 and rear 1 rods during the sequence.

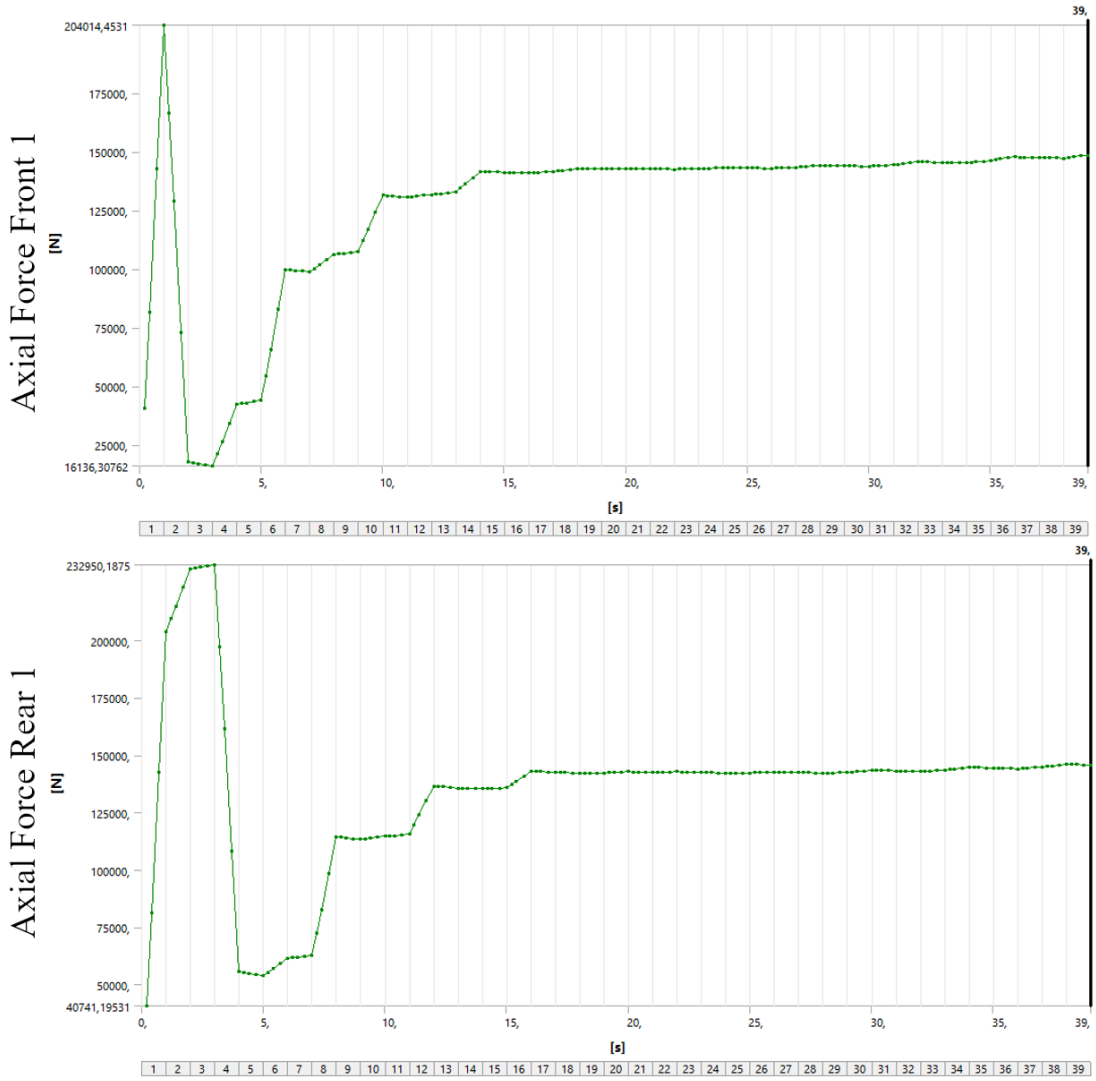

Figure 40. Tightening sequence analysis axial force of front 1 and rear 1 rods during the sides-centre sequence.

The rods stop getting affected by the sequence on steps 14 (F4) and 16 (R4) for front and rear rods respectively. Front and rear rod tightening can be seen affecting each other dramatically less compared to rods in the same row. Figure 41 shows how the axial force changes in the front 10 and rear 10 rods during the sequence.

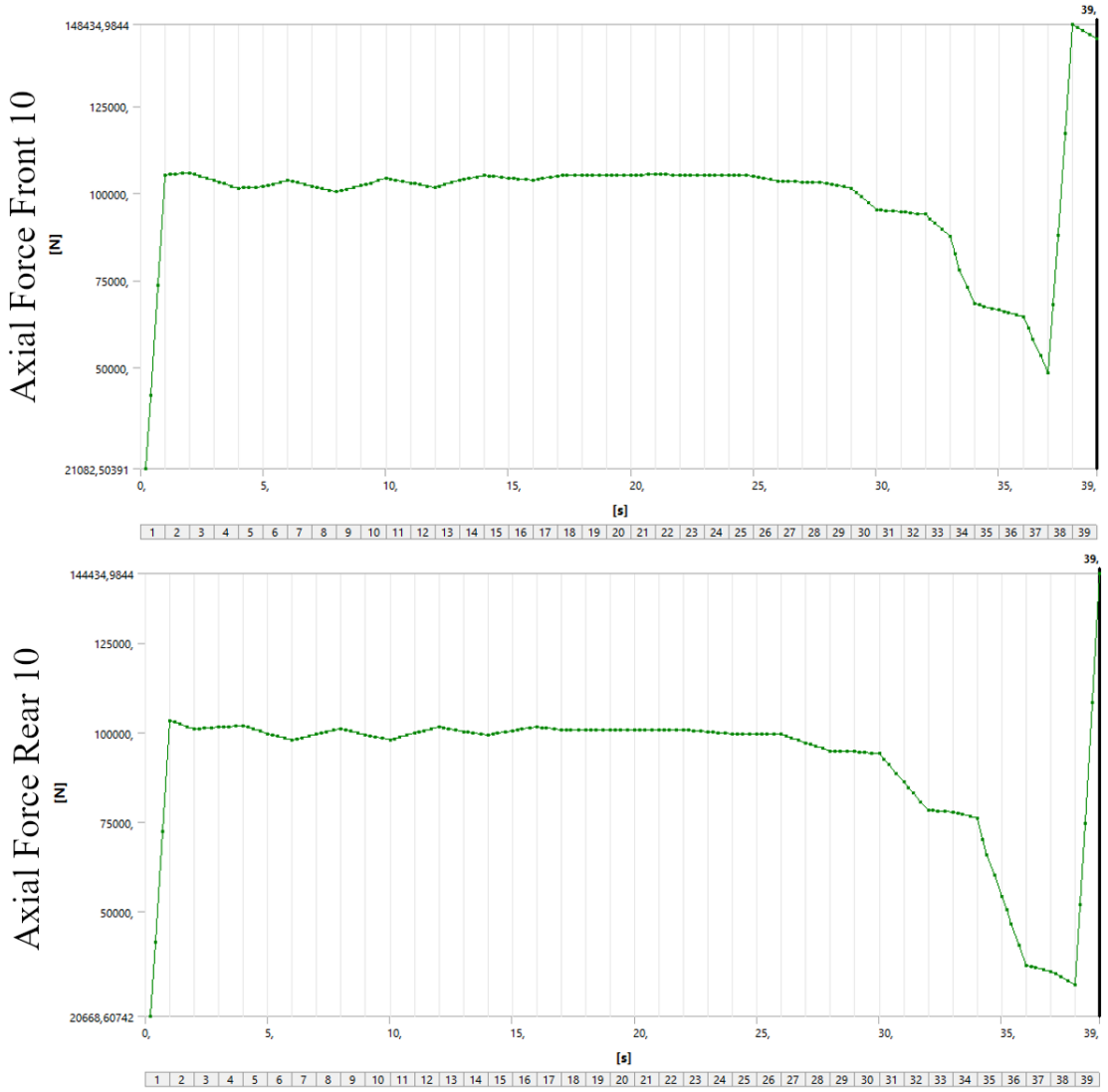

Figure 41. Tightening sequence analysis axial force of front 10 and rear 10 rods during the sides-centre sequence.

The rods, which are the last to be tightened in the sequence, start to lose their tension to surrounding rods on steps 30 (F8) and 31 (R12) of the sequence for front and rear respectively. The beginning of the sequence shows rising and lowering of the preload most likely due to the structure rocking slightly as tightening alternates between front and rear rods. Table 3 shows how iterating the sequences affect their load variance.

Table 3. Maximum and minimum load values compared to the average for each iteration step.

	Maximum and minimum load value compared to average [%]					
Iteration	**Center-sides**		**Sides-center**		**SH rods**	
	Hanger rod	SH rod	Hanger rod	SH rod	Hanger rod	SH rod
Initial	+41.3; -28.4	+63.6; -44.4	+41.3; -28.4	+63.6; -44.4	+2.9; -1.1	+24.2; -34.5
1	+304.8; -130.1	+336; -137,.4	+28; -17.1	+50.5; -40.5	+2.8; -2.1	+9.4; -23.5
2	+21.2; -50.6	+45.3; -49.3	+20.7; -10.4	+43; -40.6	+3.4; -2.5	+5.2; -10.5
3	+6.9; -15	+29.5; -32.8	+15.1; -6.2	+37.1; -38.7	+4.1; -3.1	+3.8; -6.8
4	-	-	+8; -2.6	+29.7; -35.9	-	-
5	-	-	+2.9; -1.1	+24.2; -34.5	-	-

As can be seen in the table, tightening the hanger rods lowers their load variance. When SH rods are tightened the preload variance of the hanger rods increases slightly. Further iterations could be conducted to reduce the variance even further, but this would take time unless a more automated solution is implemented. Also, the accuracy of tightening to specific tension values in real world applications would become a limiting factor.

5.3 Temperature effect analysis

The front and rear rods have only a slight difference in load values (rear rods experience less loads compared to front rods) while having the same load distribution shapes. Thus, only the front rod load distributions are shown in this section. Figure 42 and Figure 43 show how dependent the front rods' load distribution is to temperature in case 1. Figure 44 and Figure 45 show the equivalent in case 2.

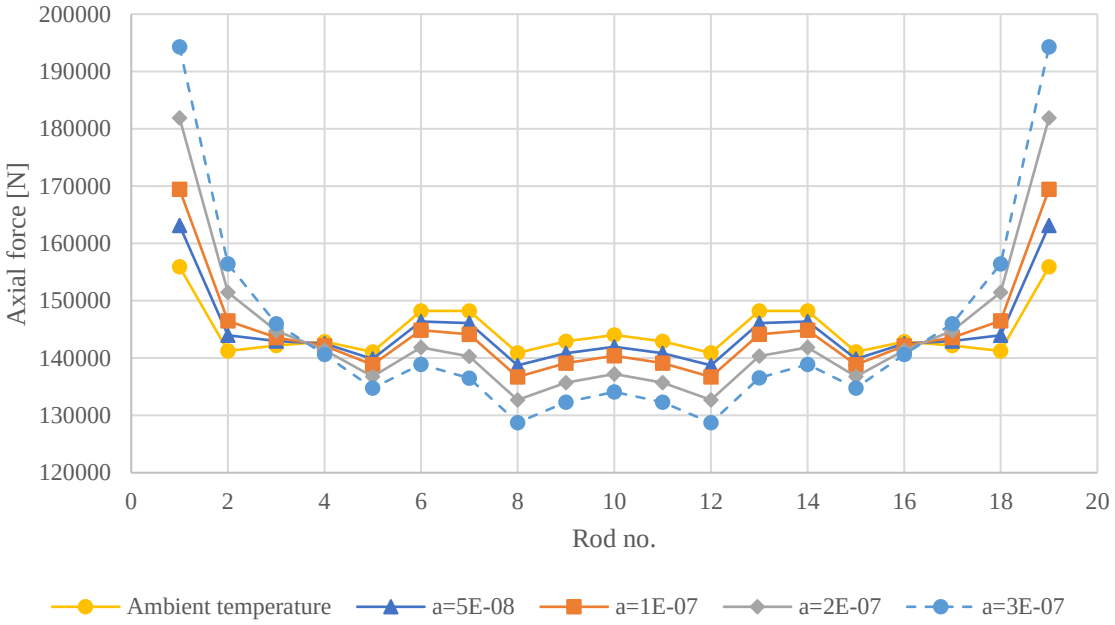

Figure 42. Load distribution temperature dependence of front rods (Case 1).

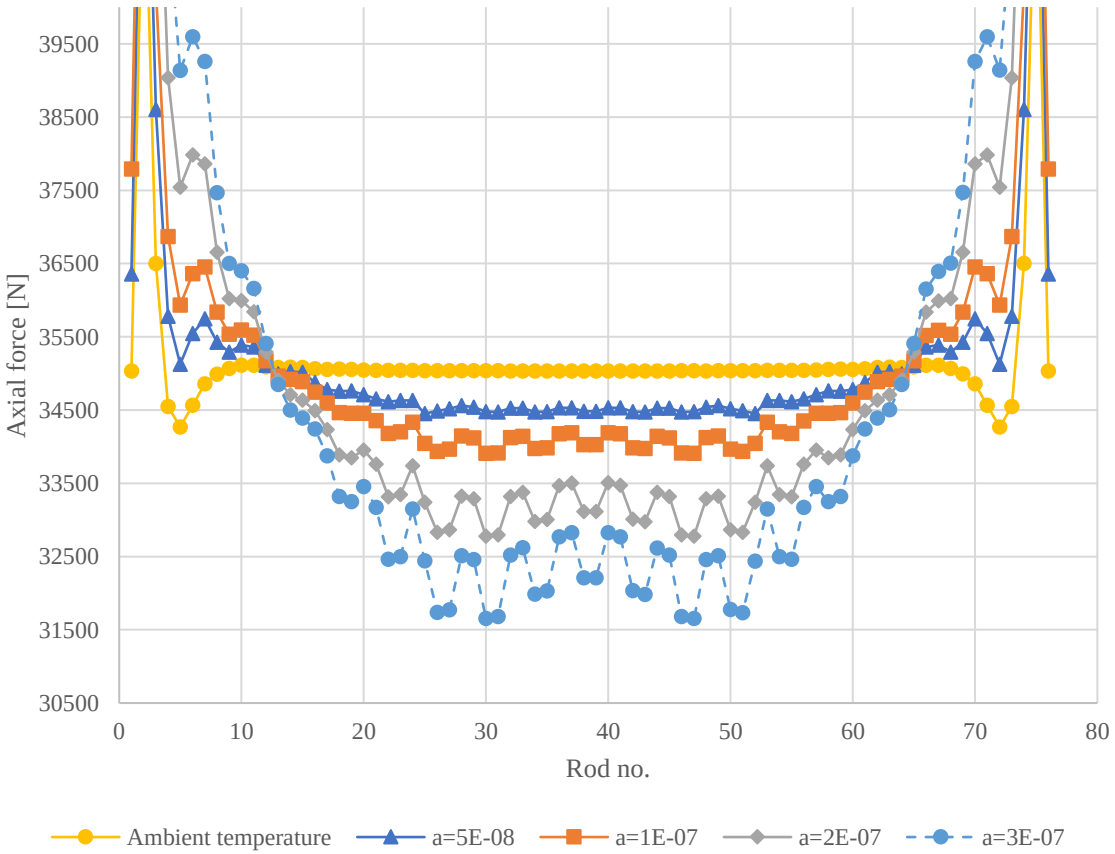

Figure 43. Load distribution temperature dependence of front SH rods (Case 1).

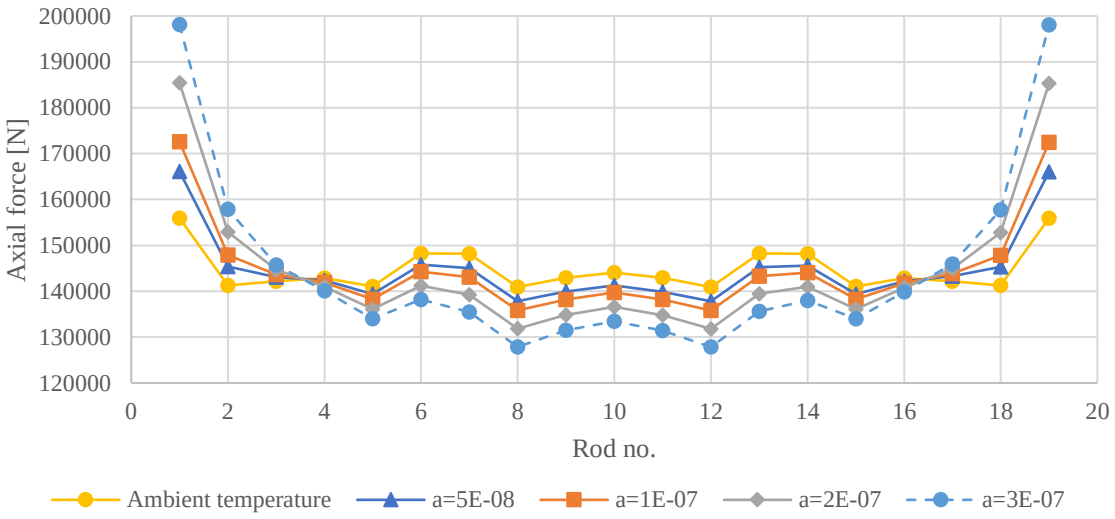

Figure 44. Hot headers load distribution temperature dependence of front rods (Case 2).

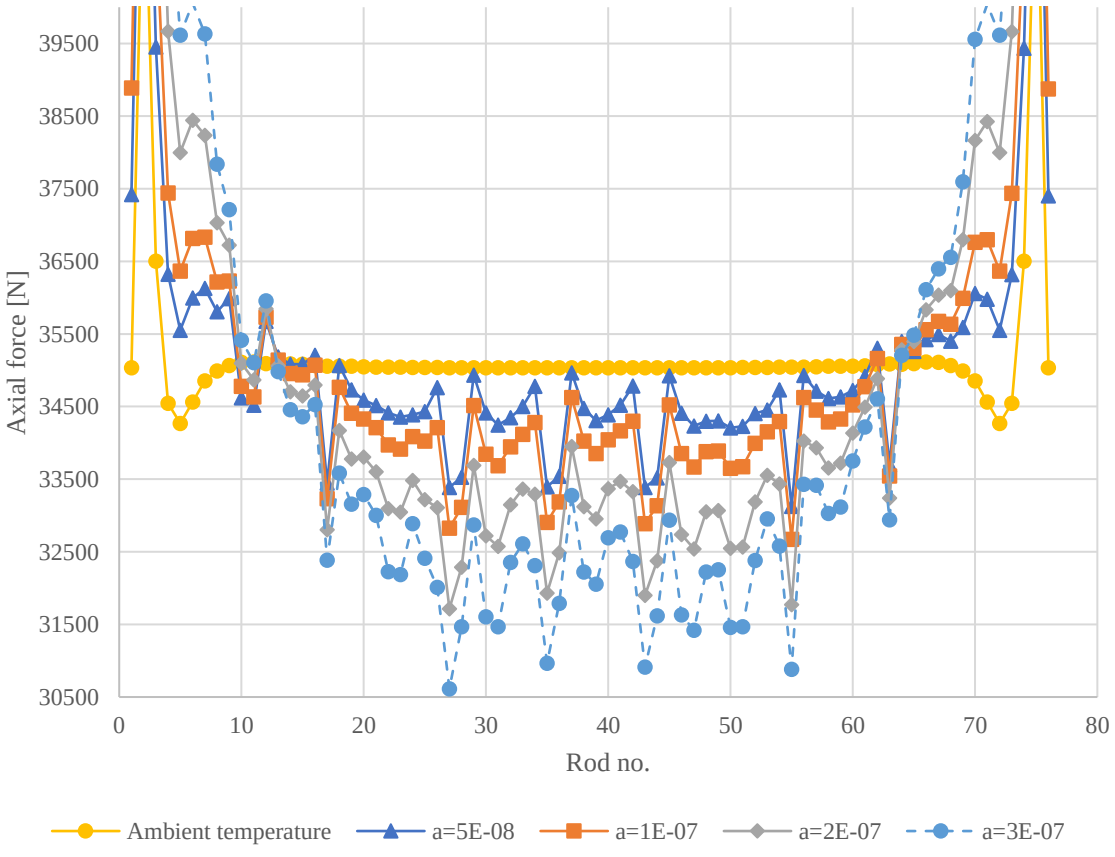

Figure 45. Hot headers load distribution temperature dependence of front SH rods (Case 2).

In both cases, the load redistribution occurs by moving the loads from the centre towards the sides in both hanger and SH rods. Load values of both the hanger rods and SH are noticed to remain almost unchanging somewhere in the middle between the 3rd and 4th side most rods, acting as a line dividing the rods to those which experience decreasing load values (inner) and those of which load values increase (outer). As the temperature range (function of *a*) increases, so does the amount of load redistributed from centre towards the sides. In the hot headers' case, the hanger rod load distribution has a similar shape compared to case 1, but a major difference is noticed in the SH rod load distribution, where their loads dip near the hanger rods and the load distribution is asymmetric.

5.4 Generalized results

The static indeterminacy analysis found that movement transfer from a swinging superheater element to hanger rods is prevented by the header's stiffness. The headers also cause most of the inaccuracy in obtaining locations of ash weights, thus reducing their stiffness on the structure is the most effective way of increasing the accuracy.

Tightening multiple rods simultaneously with hydraulic tensioning prevents the use of tailored pretension values for each tightened rod. This was seen in the tightening sequence analysis where four SH rods were tightened in each step of the sequence which led to the front rods having higher loads compared to the rear rods post-tightening.

Based on the temperature effect analysis, considering the tendency of the structure having preloads increase nearer to the sides and decrease near the center, creep can be considered a benefit as it would equalize the differences in rod loads. This would however require the penthouse temperature distribution to result in larger creep strain rates on the rods with higher loads compared to the looser ones.

6 Discussion

This section lists answers to the research questions based upon findings of the study, examines the reliability and validity of the analyses, and what could be studied regarding the topic in the future.

6.1 Answers to the research questions

What causes preload loss of hanger rods post-tensioning?

- The most likely culprit resulting in major loosening of singular rods is the incorrect installation of the double nut which leads to rotational loosening. The locking nut might be left untightened due to human error for example.
- Differential thermal expansion of the rods causes the loads of rods with longer lengths inside the penthouse insulation and experiencing higher temperatures to start pathing towards the shorter rods and rods experiencing smaller temperatures.
- Contrary to section 2.3.2 last paragraph, even if temperature was uniform inside the penthouse, there would be load pathing from the center most rods towards the rods nearer to the boiler columns when boiler is started up. This is due to the Young's modulus decreasing as material temperature increases inside the penthouse which results in larger deflections of the intermediate beams and headers.

What kind of effect does the tightening sequence have on post-tensioning condition?

- As was seen in Figure 40 and Figure 41, the hanger rods' load changes even when other rods are tensioned. In the sides-center sequence of the tightening sequence analysis, the side most rods were loosened from their initial load to a fraction of the average. As the sequence progressed towards the center of the structure, their loads started approaching the average via load pathing from the center to the sides which

occurred due to elastic interactions. After the sequence it had settled very close to the average.

- Tightening only a single rod when it is found loosened is difficult because its surrounding rods start losing their load via the elastic interactions as a result.

What kind of effect does the stiffness of the tertiary beams and intermediate beams have on post-tensioning condition?

- The load distribution of the rods was found to be dependent upon the deflections of the boiler beams, intermediate beams, and the headers which in turn depend on their stiffnesses and distance between supports.
- Especially the free edges of the intermediate beams were found to result in lower loads on their nearest SH rods. If a sectioned intermediate beam is used, then the amount of these free edges increases thus having more variance in the SH rod loads.

How does the penthouse environmental condition affect the hanger rods?

- The penthouse temperature increase as the boiler starts causes thermal expansion of the rods and lowers the Young's modulus of parts inside it. Depending on the temperature distribution and the temperature affected lengths of the rods, load distribution is affected.
    - It should be noted that a reversal of these effects occurs when temperature decreases, which might cause incorrect interpretation of the operational tension condition during shutdown maintenance.

How should a structure where the load on each hanger rod is verifiable be created?

- The tension of each rod can be accurately measured using percussion-based methods such as Wang F. & Song (2020), which work similarly to how for example guitar strings are tuned.

- The proper installation of the double nuts should be ensured so that the structure achieves proper resistance against rotational loosening (see section 2.1.3).
    - The double nut method causes difficulties in achieving a desired overall tension and if hydraulic tensioning is desired, it's only possible for the bottom nut
    - Only a small locking effect is achieved if a single nut is tightened to the desired preload and then another nut is tightened similarly on top of it.
- If the double nut cannot be installed so that the load distribution variance is satisfactory and a proper locking effect is achieved, other rotational loosening prevention methods should be considered (see section 2.1.3).
- Tightening the hanger rods should be conducted by first examining the beam deflections and then tightening from lowest deflection with low preload and progressing towards locations with larger deflections while increasing the amount of tightening towards the average value. In the superheater case this means tightening the rods nearest to the boiler columns first and progressing towards the center while alternating between opposite sides of the boiler and between the front and rear rods (see Appendix 4 column "Sides-center sequence").
- Tightening the SH rods requires using higher preloads for SH rods nearest to the intermediate beam free edges and increasing preloads the further away the SH rod is from a hanger rod. The hanger rods should be tightened before the SH rods. Note that tightening the SH rods slightly worsens the hanger rod load distribution (see *Table 3* column "SH rods").
- Tightening the rods using hydraulic tensioning allows much more accurate control of tension for each rod, which is required if a predetermined tightening sequence and preload values are needed to obtain a uniform load distribution. If every rod were tightened simultaneously using hydraulic tensioning, a uniform load distribution could be easily obtained. However, this is not realistic as there are hundreds of rods inside the penthouse, and only tightening a few rods simultaneously at a time in a sequence prevents utilizing the tailored preload values needed for each rod as was found in the tightening sequence analysis.

6.2 Comparison and connections with former research

Pöllänen (2019) studied ways of measuring the hanger rod loads and concluded that accurate measurements need a uniform load distribution. This study built on that research by examining what causes rod loads to change and how a uniform load distribution could be achieved.

The elastic interaction effect studied in 2.2.1 seemed to act in a similar way even on suspended bolted joints, however contrary to the research referenced, where only the stiffness of the elements in contact needed to be considered, the phenomenon in the hanger rod structure is much more complex, causing difficulty in obtaining analytical solutions.

6.3 Reliability and validity

Analysis simplifications' effects on validity of results:

- Line bodies were used to save on computation time. Through thickness stress distribution on elements and cross-sectional deformation were not needed for the analyses so effect on validity is acceptable. Deflection of bent header pipes were affected as the line model had them connect to the cross-section centre of the headers instead of the outer surface like in the real structure. This resulted in slightly less stiffness than the real structure and thus also affected the accuracy of the result of the 'straight header pipes removed' part of the static indeterminacy analysis. Line bodies and the coarse mesh prevented analysing local stresses which could experience creep strain in the real structure.
- The analyses did not consider the effect of the furnace roof to furnace front and side wall connection. Load pathing through these depend on the tension condition of the furnace wall hanger rods, which were not part of the thesis' scope.

- The static indeterminacy analysis did not consider the hanger rod supporting beam structure.
- The analyses did not consider the effects of load pathing from one superheater to another via the furnace roof and risers.
- The temperature effect analysis had the whole hanger rod in elevated temperature as opposed to the real structure, where a part of the rod is outside the insulation layer. This should not affect the reliability of the results as they are dependent on the differential thermal expansion instead of the absolute expansion values. Also the Young's modulus used was the same for every part in elevated temperatures although there was temperature difference between the sides and centre. Pressure inside the headers and connecting piping was not accounted for, this resulted in lower stiffness compared to the real structure.
    - The temperature distribution used in the analysis was completely made-up just to see the kind of effects different temperature ranges had on the structure. Tests have yet to be done to find out the real temperature distribution inside the penthouse during boiler operation.

Overall, the absolute values were not of interest in the analyses whereas the phenomena affecting the structure were, and the simplifications mainly affected the accuracy of the simulation. Thus, the validity and reliability of the analyses are acceptable.

6.4 Topics for future research

The tightening sequence analysis found that the load distribution variance of the suspended bolted joint could be improved by iterating the sequence. However, the iterations took quite a long time, and their results only applied to the specific structure. The literature review found that prior research has been conducted on tightening algorithms for flanged joints. Therefore, the feasibility of similar algorithms for determining elastic interactions and thus optimal tightening sequences for suspended bolted joints could be studied. If feasible, they could enable fast calculations of the optimal tightening sequence and preload requirement

for different hanger rod arrangements, cross-section stiffnesses, and distances between supports.

Another way of achieving uniform load distribution is to allow plasticization of the hanger rods under higher load, thus transferring load from them towards looser rods. Achieving this would require forgoing safety margins in the dimensioning phase of the rods so that plasticization occurs when a rod exceeds the equally distributed average load, the calculation of which would need accurate knowledge of the hanged weights. This kind of dimensioning might be problematic to apply due to standard/customer requirements. As loads would exceed the yield limit of the material, the effect of creep would become increasingly prevalent, the effect of which could be reduced via material selection for better creep resistance or by lowering the temperature experienced by the rods.

The swinging of the superheater elements was listed as one of the research problems but was found to not be dependent upon the hanger rod tension condition as much as expected. The stiffness of the superheater element itself against sootblower steam induced excitation should be studied to find how increasing superheater sizes as demand for ever larger boilers grows may worsen the swinging problem in the future, and what could be done to improve the structure so that the effect is reduced.

The variance of temperature inside the penthouse could be studied, so that the load redistribution due to thermal expansion and relaxation could be compensated for already before boiler startup, and to predict the reversal of the thermal effects when penthouse cools down so that incorrectly interpreting that a rod was loose even during boiler operation could be avoided.

References

ABASOLO, M., AGUIRREBEITIA, J., AC, R.R. and FERNANDEZ DE BUSTOS, I., 2011. A Tetraparametric Metamodel for the Analysis and Design of Bolting Sequences for Wind Generator Flanges. Journal of Pressure Vessel Technology, Transactions of the ASME, 133.

BIBEL, G.D. and EZELL, R.M., 1992. An Improved Flange Bolt-Up Procedure Using Experimentally Determined Elastic Interaction Coefficients. Journal of Pressure Vessel Technology, 114(4), pp. 439-443.

BIBEL, G. and EZELL, R., 1996. Bolted flange assembly: Preliminary elastic interaction data and improved bolt-up procedures. Bulletin - Welding Research Council, (408).

BICKFORD, J.H., 1995. An introduction to the design and behavior of bolted joints. 3 edn. New York: Dekker.

BIRD, J. and ROSS, C., 2020. Mechanical engineering principles. 4 edn. Abingdon, Oxon: Routledge.

BOLT SCIENCE, 2021a-last update, Preload Loss from Embedding in Bolted Joints, [Website]. Available: https://www.boltscience.com/pages/embedding.htm [Cited 20.5., 2022].

BOLT SCIENCE, 2021b-last update, Preload Loss from Stress Relaxation, [Website]. Available: https://www.boltscience.com/pages/stress-relaxation.htm [Cited 31.5., 2022].

BOLT SCIENCE, 2021c-last update, The Use of Two Nuts to Prevent Self Loosening, [Website]. Available: https://www.boltscience.com/pages/twonuts.htm [Cited 7.10., 2022].

EVANS, R.W. and WILSHIRE, B., 1993. Introduction to creep. London: Institute of Materials.

GODDARD, D.L. and BIBEL, G., 1994. Achieving a Selected Load Distribution in the Bolted Joint of a Cylinder Head of Highly Variable Stiffness and Contact Geometry, International Congress and Exposition.

GONG, H., DING, X., LIU, J. and FENG, H., 2021. Review of research on loosening of threaded fasteners. Friction, 10(3), pp. 335-359.

GONG, H., LIU, J. and FENG, H., 2022. Review on anti-loosening methods for threaded fasteners. Chinese Journal of Aeronautics, 35(2), pp. 47-61.

GONZÁLEZ-VELÁZQUEZ, J.L., 2020. Mechanical Behavior and Fracture of Engineering Materials. 1 edn. Cham: Springer International Publishing.

HESS, D.P., 2022. Torque Balance, Primary Locking and Loosening in Tensioner-Assembled Bolted Joints. Journal of failure analysis & prevention., 22(2), pp. 542-549.

ISO 898-2, 2012. Mechanical properties of fasteners made of carbon steel and alloy steel - Part 2: Nuts with specified property classes - Coarse thread and fine pitch thread, [Standard].

JAGLINSKI, T., NIMITYONGSKUL, A., SCHMITZ, R. and LAKES, R., 2007. Study of Bolt Load Loss in Bolted Aluminum Joints. Journal of Engineering Materials and Technology-transactions of The Asme - J ENG MATER TECHNOL, 129.

JIANG XIANGJUN, LI, Z., WANG, Y. and PAN FENGQUN, 2019. Self-loosening behavior of bolt in curvic coupling due to materials ratcheting at thread root. Advances in Mechanical Engineering, 11(5), pp. 597-608.

JUNKER, G.H., 1969. New Criteria for Self-Loosening of Fasteners Under Vibration.

KAKIRDE, A. and DRAVID, S., 2018. Study of Vibration Loosening of Bolted Joints-A Review. Journal for Advanced Research in Applied Sciences, 5(1), pp. 36-45.

KAKIRDE, A. and DRAVID, S., 2017. A review on loosening of bolted joints. International Journal of Advance Research in Science and Engineering, 6(1), pp. 988-997.

KASEI, S., ISHIMURA, M. and OHASHI, N., 1988. On Self-loosening of Threaded Joints in the Case of Absence of Macroscopic Bearing-surface Sliding; Loosening Mechanism under Transversely Repeated Force. Journal of the Japan Society for Precision Engineering, 54(7), pp. 1381-1386.

KASSNER, M.E., 2009. Fundamentals of creep in metals and alloys. 2 edn. Amsterdam: Elsevier.

KIM, B.G., REMPE, J., KNUDSON, D., CONDIE, K. and SENCER, B., 2012. In-Situ Creep Testing Capability for the Advanced Test Reactor. Nuclear Technology, 179, pp. 413-428.

LI, Y., LIU, Z., WANG, Y., CAI, L. and XU, W., 2019. Research on preload of bolted joints tightening sequence-related relaxation considering elastic interaction between bolts. Journal of Constructional Steel Research, 160, pp. 45-53.

LI, Z., CHEN, Y., SUN, W., JIANG, P., PAN, J. and GUAN, Z., 2021. Study on self-loosening mechanism of bolted joint under rotational vibration. Tribology International, 161, pp. 107074.

LIU, J., OUYANG, H., FENG, Z., CAI, Z., LIU, X. and ZHU, M., 2017. Study on self-loosening of bolted joints excited by dynamic axial load. Tribology International, 115, pp. 432-451.

LIU, J., OUYANG, H., PENG, J., ZHANG, C., ZHOU, P., MA, L. and ZHU, M., 2015. Experimental and numerical studies of bolted joints subjected to axial excitation. Wear, 346.

METSÄ FIBRE OY, 2022-last update, Towards fossil-free mills, [Website]. Available: https://www.metsafibre.com/en/media/Stories/Pages/Towards-fossil-free-mills.aspx [Cited 21.2., 2022].

NASSAR, S., YANG, X., GANDHAM, S. and WU, Z., 2011. Nonlinear Deformation Behavior of Clamped Bolted Joints Under a Separating Service Load. Journal of Pressure Vessel Technology, 133, pp. 021001.

NECHACHE, A. and BOUZID, A., 2007. Creep analysis of bolted flange joints. International Journal of Pressure Vessels and Piping, 84(3), pp. 185-194.

PEARSON, S.R., SHIPWAY, P.H., ABERE, J.O. and HEWITT, R.A.A., 2013. The effect of temperature on wear and friction of a high strength steel in fretting. Wear, 303(1), pp. 622-631.

PÖLLÄNEN, I., 2019. The efficiency and damage control of a recovery boiler, [Dissertation].

SEARS, G. and KING, D., 2004. Joint integrity management of critical flanges. International Journal of Pressure Vessels and Piping, 81(6), pp. 513-519.

VAKKILAINEN, E., 2005. Kraft recovery boilers – Principles and practice. Valopaino Oy.

WANG, F. and SONG, G., 2020. Bolt-looseness detection by a new percussion-based method using multifractal analysis and gradient boosting decision tree. Structural Health Monitoring, 19(6), pp. 2023-2032.

WANG, Y.-., WU, J.-., LIU, H.-., KUANG, K., CUI, X.-. and HAN, L.-., 2017. Analysis of elastic interaction stiffness and its effect on bolt preloading. International Journal of Mechanical Sciences, 130, pp. 307-314.

WICKER, K., 2003. A smarter way to remove slag. Power, 147.

WILSHIRE, B. and BATTENBOUGH, A.J., 2007. Creep and creep fracture of polycrystalline copper. Materials Science and Engineering: A, 443(1), pp. 156-166.

YANG, X., NASSAR, S., WU, Z. and MENG, A., 2012. Nonlinear Behavior of Preloaded Bolted Joints Under a Cyclic Separating Load. Journal of Pressure Vessel Technology, 134, pp. 011206.

Appendix 1. Cross-sections used in the analyses.

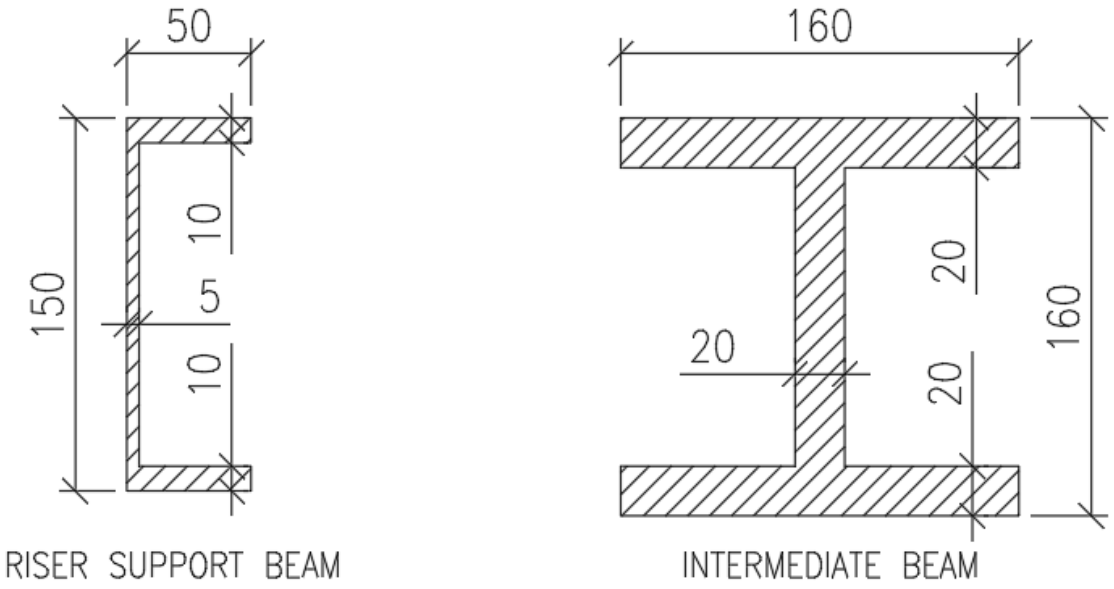

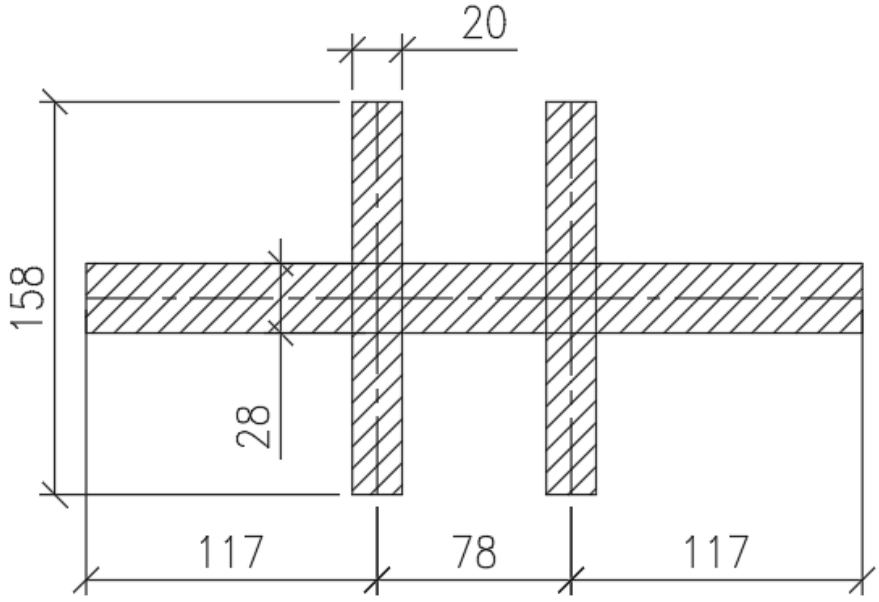

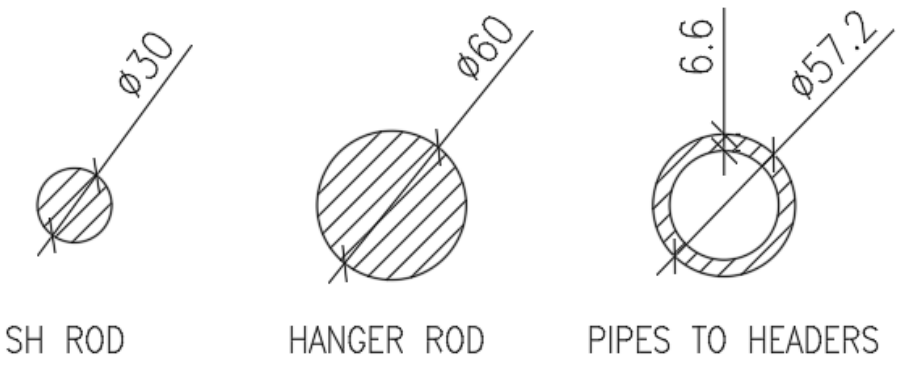

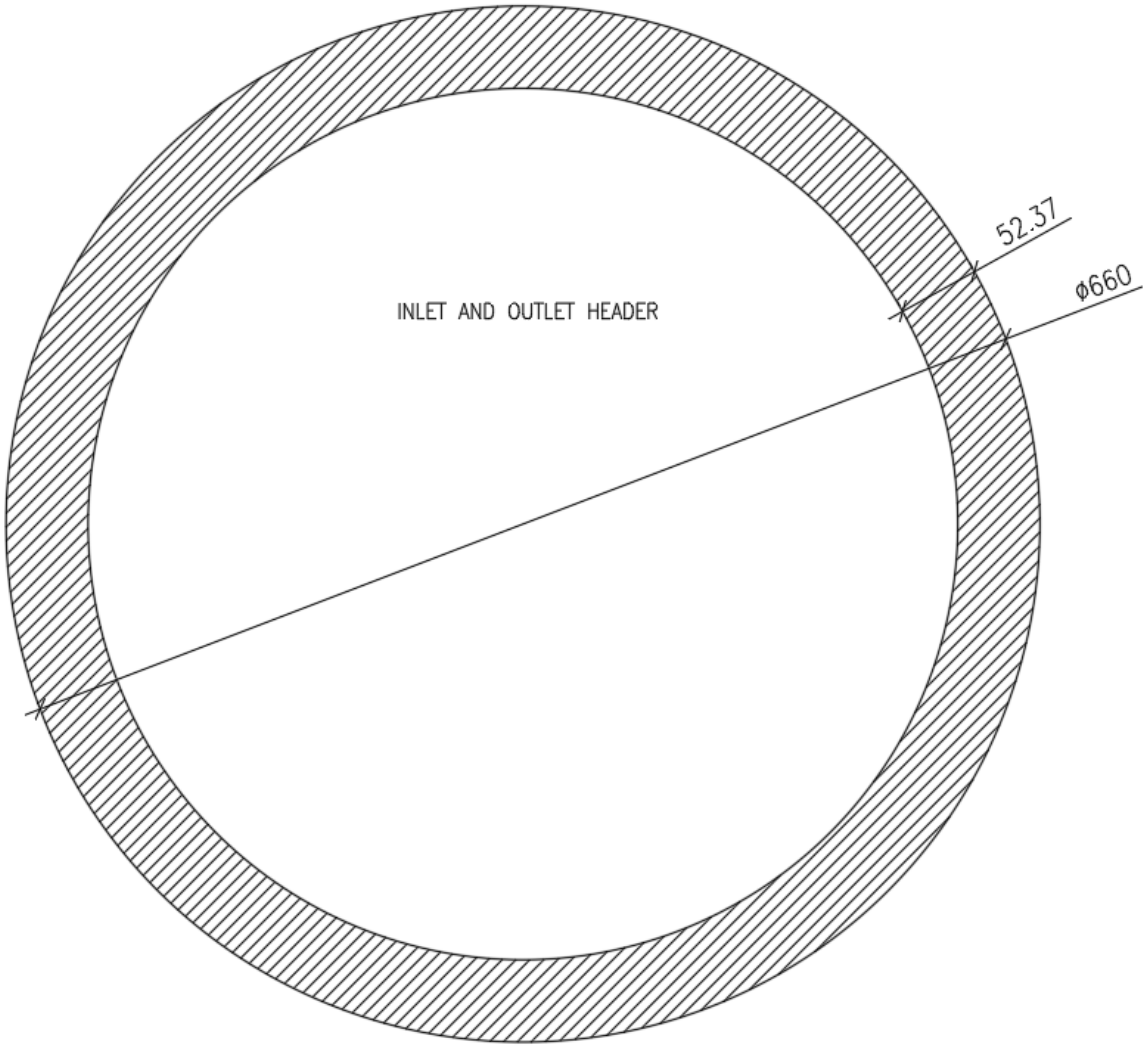
52.37
ϕ660
INLET AND OUTLET HEADER

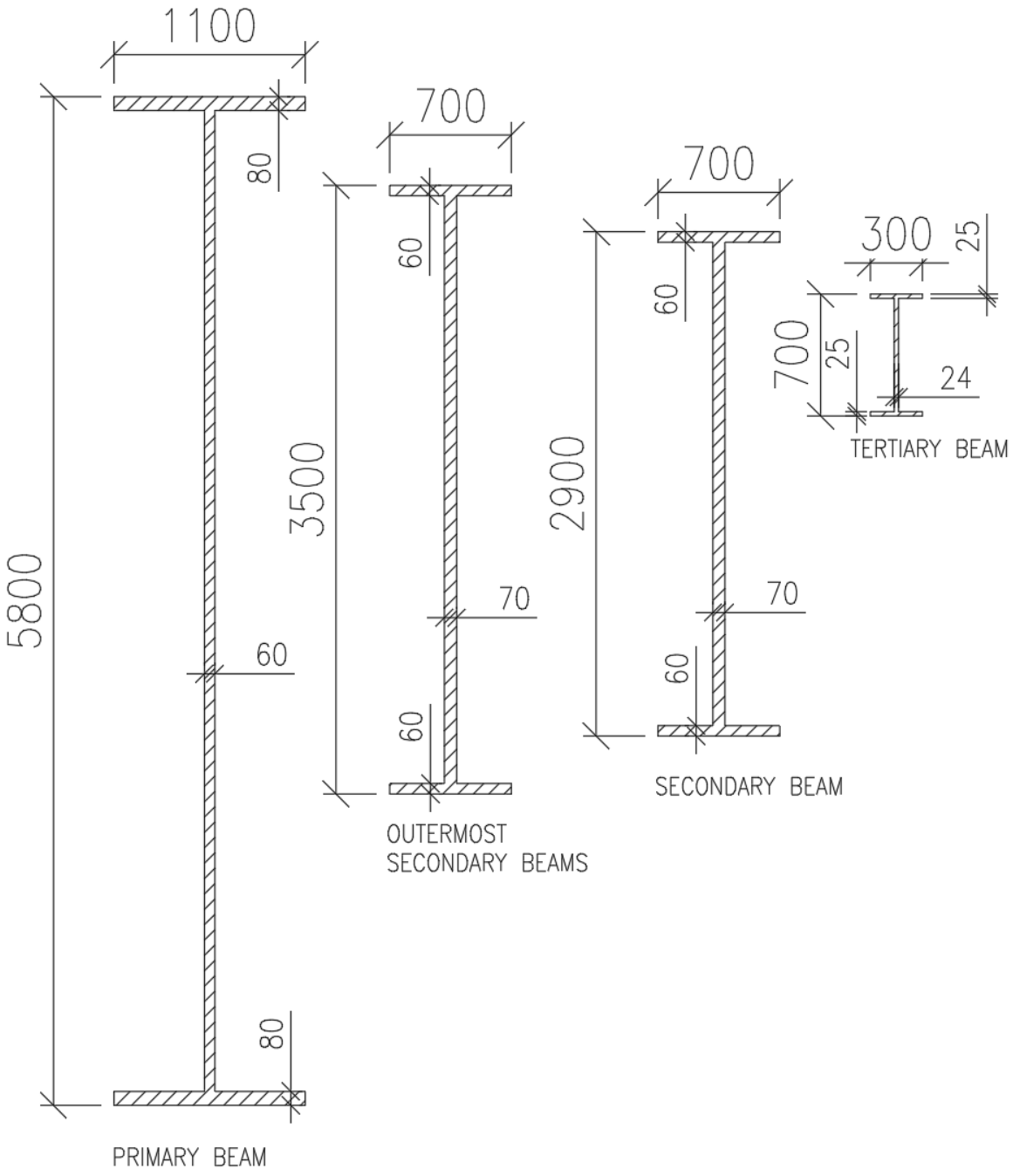
1100
80
5800
60
80
PRIMARY BEAM
700
60
3500
70
60
OUTERMOST
SECONDARY BEAMS
700
60
2900
70
60
SECONDARY BEAM
300
25
700
25
24
TERTIARY BEAM

Appendix 2. Structure and dimensions of the analysis models.

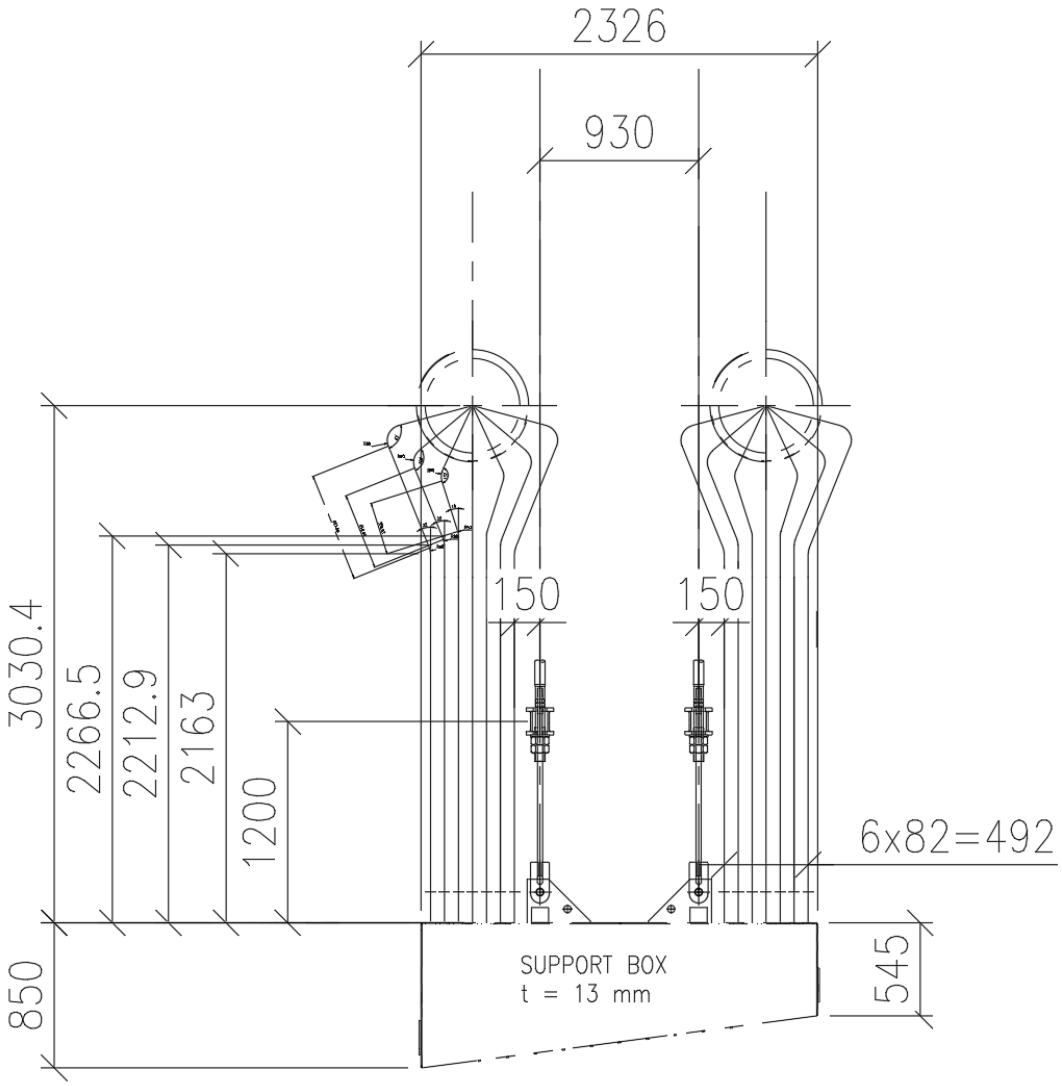

Appendix 2.1 Right hand side view of the structure and its geometry (facing the negative Z-direction).

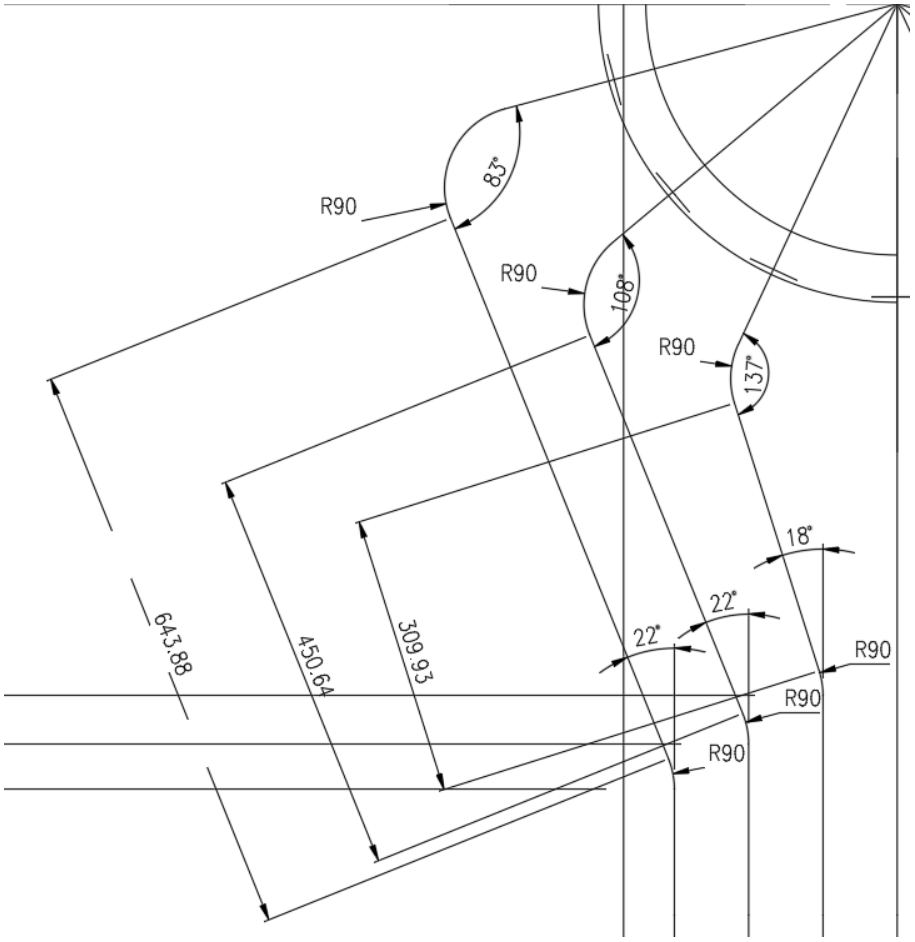

Appendix 2.2 Bends of pipes to inlet and outlet headers.

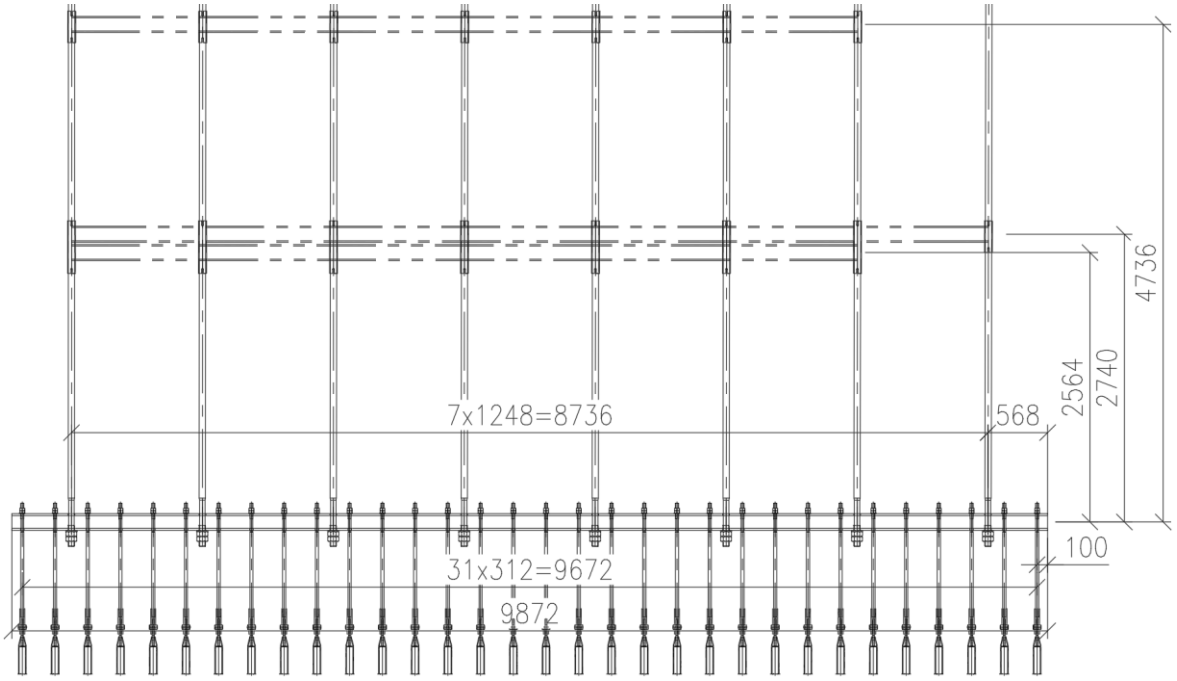

Appendix 2.3 Static indeterminacy analysis dimensions and geometry of the front rods.

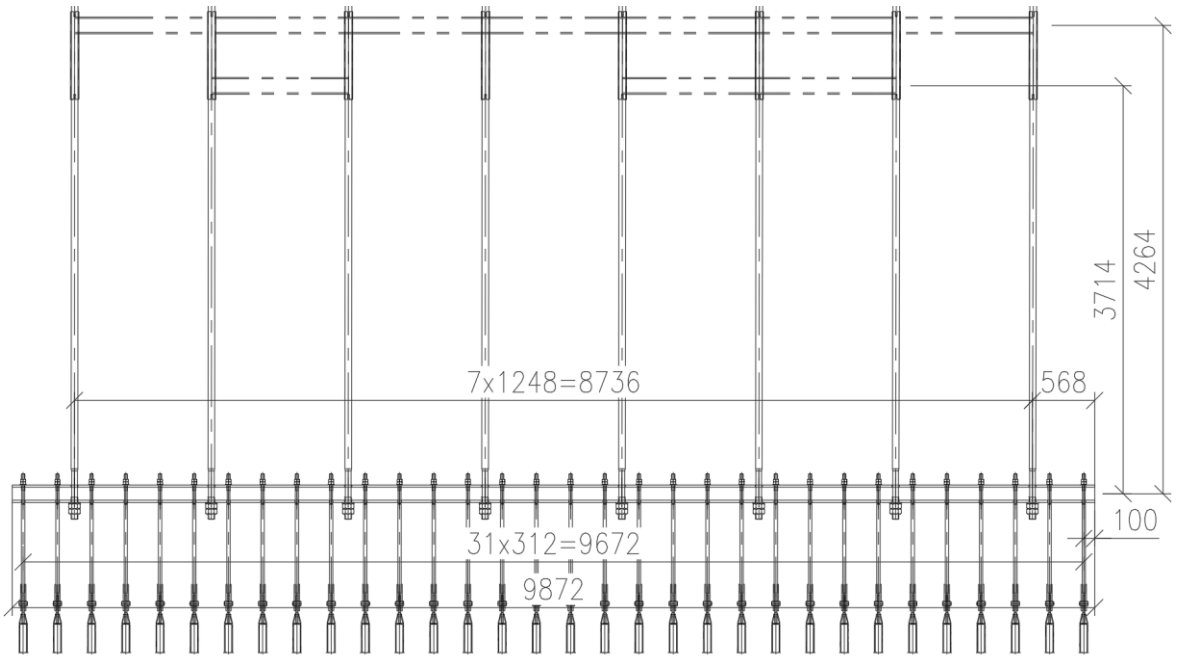

Appendix 2.4 Static indeterminacy analysis dimensions and geometry of the rear rods.

Appendix 3. Tightening sequence and temperature effect analysis boiler beam geometry and loads.

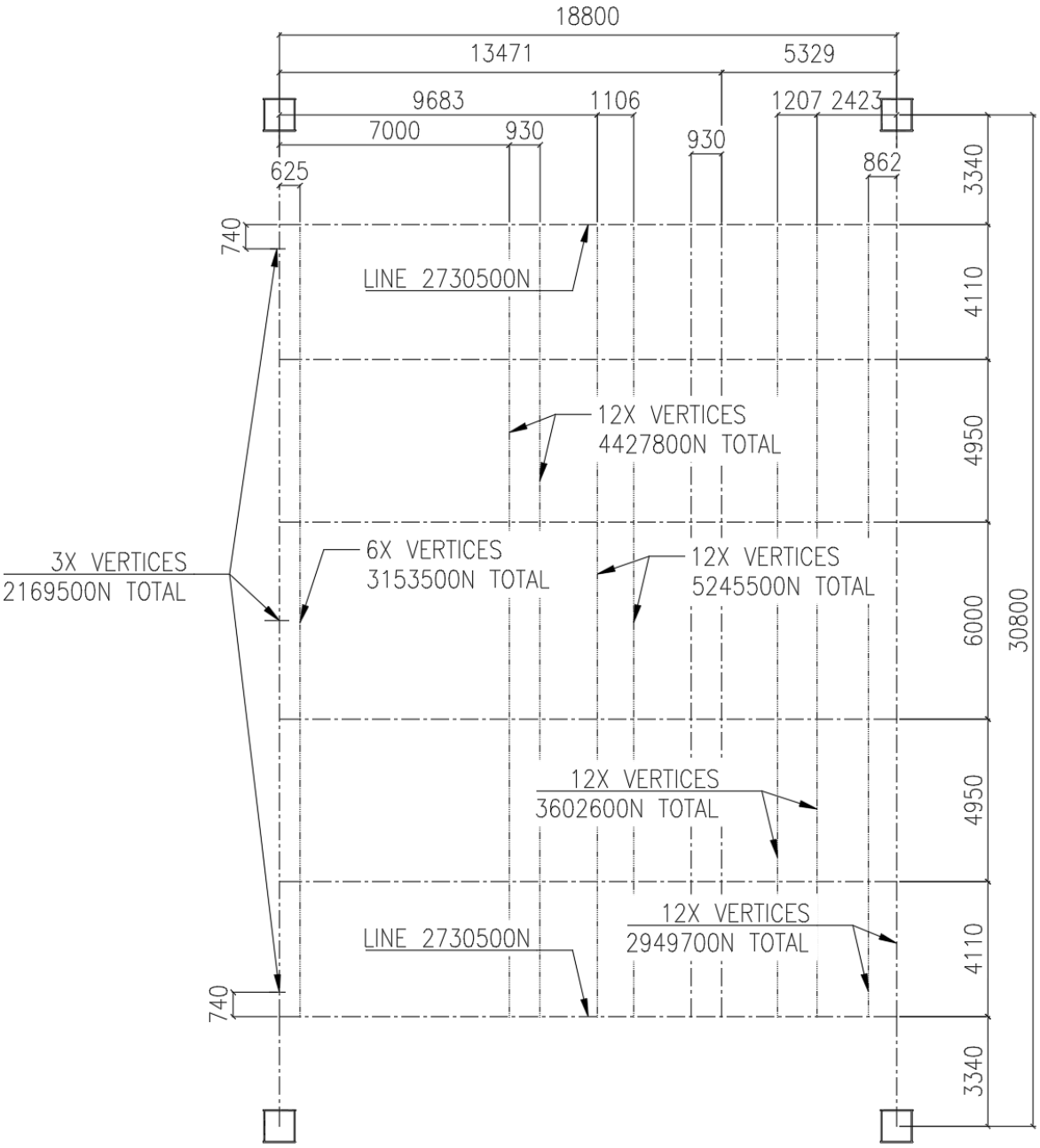

Appendix 4. Tightening sequences and preload values of each sequence's final iteration.

Step	**Center-sides sequence**	Preload [N]	**Sides-center sequence**	Preload [N]	**SH rod sequence**	Preload [N]
1	Beam loads, gravity and platen weights applied					
2	F 10	407900	F1	16600	F 2 - 18 ; R 2 - 18	143000
3	R 10	411700	R19	25800	F 1 & 19 ; R 1 & 19	145000
4	F 9	343700	R1	53600	SHF 1 & 76 ; SHR 1 & 76	39000
5	R 11	342300	F19	43000	SHF 2 & 75 ; SHR 2 & 75	34500
6	R 9	296700	F2	87000	SHF 3 & 74 ; SHR 3 & 74	34300
7	F 11	293600	R18	95300	SHF 4 & 73 ; SHR 4 & 73	31700
8	F 8	300400	R2	104700	SHF 5 & 72 ; SHR 5 & 72	29400
9	R 12	298600	F18	95400	SHF 6 & 71 ; SHR 6 & 71	31900
10	R 8	266000	F3	119200	SHF 7 & 70 ; SHR 7 & 70	34800
11	F 12	270600	R17	128500	SHF 8 & 69 ; SHR 8 & 69	33700
12	F 7	277700	R3	135500	SHF 9 & 68 ; SHR 9 & 68	31700
13	R 13	276600	F17	125200	SHF 10 & 67 ; SHR 10 & 67	34000
14	R 7	250600	F4	141900	SHF 11 & 66 ; SHR 11 & 66	36700
15	F 13	257500	R16	151200	SHF 12 & 65 ; SHR 12 & 65	35300
16	F 6	236700	R4	156100	SHF 13 & 64 ; SHR 13 & 64	33100
17	R 14	235100	F16	146000	SHF 14 & 63 ; SHR 14 & 63	35000
18	R 6	218800	F5	158100	SHF 15 & 62 ; SHR 15 & 62	37600
19	F 14	224000	R15	165700	SHF 16 & 61 ; SHR 16 & 61	35300
20	F 5	186000	R5	166400	SHF 17 & 60 ; SHR 17 & 60	32000
21	R 15	189000	F15	158900	SHF 18 & 59 ; SHR 18 & 59	32500
22	R 5	176900	F6	168300	SHF 19 & 58 ; SHR 19 & 58	33300
23	F 15	177000	R14	174200	SHF 20 & 57 ; SHR 20 & 57	30900
24	F 4	161400	R6	173000	SHF 21 & 56 ; SHR 21 & 56	31500
25	R 16	169300	F14	167700	SHF 22 & 55 ; SHR 22 & 55	40300
26	R 4	163700	F7	181700	SHF 23 & 54 ; SHR 23 & 54	50300
27	F 16	156200	R13	186300	SHF 24 & 53 ; SHR 24 & 53	35600
28	F 3	153500	R7	182600	SHF 25 & 52 ; SHR 25 & 52	39600
29	R 17	156300	F13	179100	SHF 26 & 51 ; SHR 26 & 51	35800
30	R 3	152300	F8	197300	SHF 27 & 50 ; SHR 27 & 50	35900
31	F 17	149700	R12	201700	SHF 28 & 49 ; SHR 28 & 49	33700
32	F 2	133700	R8	194100	SHF 29 & 48 ; SHR 29 & 48	31500
33	R 18	135400	F12	191100	SHF 30 & 47 ; SHR 30 & 47	33900
34	R 2	132000	F9	193000	SHF 31 & 46 ; SHR 31 & 46	36900
35	F 18	130400	R11	198100	SHF 32 & 45 ; SHR 32 & 45	35400
36	F 1	141000	R9	180400	SHF 33 & 44 ; SHR 33 & 44	33300
37	R 19	140100	F11	175200	SHF 34 & 43 ; SHR 34 & 43	35500
38	R 1	145100	F10	148000	SHF 35 & 42 ; SHR 35 & 42	38200
39	F 19	144800	R10	144000	SHF 36 & 41 ; SHR 36 & 41	36700
40	N/A		N/A		SHF 37 & 40 ; SHR 37 & 40	34300
41	N/A		N/A		SHF 38 & 39 ; SHR 38 & 39	35200